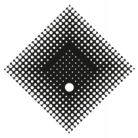
VICTORIA UNIVERSITY
MELBOURNE AUSTRALIA

Application of a multi-objective approach integrating solar-wind co-generation with response surface method to optimize zero-energy buildings

This is the Published version of the following publication

Assareh, Ehsanolah, Izadyar, Nima, Jamei, Elmira, Mobayen, Saleh, Abbasi, Majid, Mohammadi, Hassan, Agarwal, Neha and Lee, Moonyong (2025) Application of a multi-objective approach integrating solar-wind co-generation with response surface method to optimize zero-energy buildings. Applied Thermal Engineering, 265. ISSN 1359-4311

The publisher's official version can be found at https://doi.org/10.1016/j.applthermaleng.2025.125637
Note that access to this version may require subscription.

Downloaded from VU Research Repository https://vuir.vu.edu.au/49390/

Applied Thermal Engineering 265 (2025) 125637

Contents lists available at ScienceDirect

Applied Thermal Engineering

journal homepage: www.elsevier.com/locate/apthermeng

Research Paper

Application of a multi-objective approach integrating solar-wind co-generation with response surface method to optimize zero-energy buildings

Ehsanolah Assareh [a,b], Nima Izadyar [b,c,*], Elmira Jamei [b,c], Saleh Mobayen [d], Majid Abbasi [e], Hassan Mohammadi [e], Neha Agarwal [a], Moonyong Lee [a,**]

[a] School of Chemical Engineering, Yeungnam University, Gyeongsan 38541, South Korea
[b] Built Environment and Engineering Program, College of Sport, Health and Engineering (CoSHE), Victoria University, Melbourne, Australia
[c] Institute for Sustainable Industries and Liveable Cities, Victoria University, Melbourne, VIC 3011, Australia
[d] Graduate School of Intelligent Data Science, National Yunlin University of Science and Technology, Douliou, Yunlin 640301, Taiwan
[e] Department of Mechanical Engineering, Lamerd Branch, Islamic Azad University, Lamerd, Iran

ARTICLE INFO

Keywords:
Co-generation systems
Energy efficiency
Pitch Angle Control
Power generation
Solar-Wind Hybrid Systems
Wind Turbine
Zero Energy Building (ZEB)

ABSTRACT

Achieving zero energy in residential buildings is particularly challenging in hot climates due to high cooling loads and reliance on conventional energy. This study introduces a co-generation system integrating a hybrid solar-wind setup with a Modified Steam Rankine Cycle and a Reverse Osmosis desalination unit to supply electricity, thermal energy, cooling, and potable water to a 360 m2 apartment complex in Ahvaz, Iran. BEopt software was used to extract energy consumption data, while energy and exergy assessments were performed using the Engineering Equation Solver and Response Surface Method. The system achieves an Exergetic Round Trip Efficiency of 34.02 % and an Energy Efficiency of 33.05 %. It meets annual energy needs with surplus energy fed back to the grid, generating 1,672 kWh of power, 8,760 kWh of heating, and 1,279 kWh of cooling while reducing 1,334.47 tons of carbon dioxide emissions. Pitch angle control in the 5 MW wind turbine enhances electricity generation by 4 %, leading to annual outputs of 6,541,564 kWh of electricity, 14,717,841 kWh of heating, 2,023,099 kWh of cooling, and 380,858 m3 of freshwater. The system stores excess thermal regulation for heating and air conditioning energy, contributing to cost-effectiveness and ecological sustainability. This study highlights the system's ability to achieve net-zero energy, with significant reductions in carbon emissions and the provision of substantial freshwater, demonstrating its potential in extreme climates. Future studies can explore the dynamic optimization of hybrid systems, focusing on real-time energy distribution between cooling, desalination, and energy storage.

1. Introduction

A Zero-Energy Building (ZEB) can operate without relying on fossil fuels, emitting no carbon pollutants, and marking a significant advancement in sustainable building design [1–3]. Although creating a ZEB that obtains all its energy from green sources has traditionally been seen as a challenging task due to technological limitations, including the need for efficient energy storage systems [4–6], it is now becoming more achievable and realistic [7–9]. ZEBs integrate energy efficiency and on-site clean energy utilization to meet their energy needs exclusively through renewable sources within a specified timeframe [10]. By depending entirely on renewable sources, ZEBs are transforming energy practices in the construction industry and motivating more building owners to embrace these methods [11]. The need for ZEBs becomes even more urgent as the global population grows and energy demands in homes rise, making it essential to move away from dwindling traditional energy sources like gas and oil due to the increasing strain on global resources and the costs associated with fossil fuels [12]. Moreover, the ecological effects of consuming fossil fuels and the ongoing fight against global warming underscore the crucial importance of using alternative green energy sources [13–15].

* Corresponding author at: Built Environment and Engineering Program, College of Sport, Health and Engineering (CoSHE), Victoria University, Melbourne, Australia.
** Corresponding author.
E-mail addresses: nima.izadyar@vu.rdu.au (N. Izadyar), mynlee@ynu.ac.kr (M. Lee).

https://doi.org/10.1016/j.applthermaleng.2025.125637
Received 29 September 2024; Received in revised form 13 December 2024; Accepted 17 January 2025
Available online 19 January 2025
1359-4311/© 2025 The Author(s). Published by Elsevier Ltd. This is an open access article under the CC BY license (http://creativecommons.org/licenses/by/4.0/).

Nomenclature

T_0	Ambient temperature [℃]
P_0	Ambient pressure [kPa]
A	Area [m^2]
$\dot{E}x$	Exergy [kW]
v	Wind speed (m/s)
C_P	Specific heat of air and water at constant pressure [kJ/kg. K]
DNI	Direct Normal Irradiation [W/m^2]
$\dot{E}x$	Exergy [kW]
$\dot{m}$	Mass flow rate [kg/s]
s	Specific entropy [kJ/kg. K]
T	Temperature [℃]
U	Overall heat transfer coefficient [kW/m2K]
h	Specific enthalpy [kj/kg]
v_a	Air speed [m/s]
x	Salinity [ppm]
$\dot{Q}$	Heat transfer rate [kW]
W	Power [kW]
T_r	receiver surface temperature [℃]
K	The ratio of specific heats

Subscripts

Cond	Condenser
eva	Evaporator
hel	Heliostat
rec	receiver
hel	Heliostat
ch	Chemical
ph	physical
cv	control volume
tur	Turbine
i	in
e	out
ST	Super heater
Eco	Economizer

Abbreviations

CRF	Capital Recover Factor
ERTE	Exergy round trip efficiency [%]
N	Number
RSM	Response surface method
RO	Reverse Osmosis
BEopt	Building Energy Optimization Tool
OSG	Over Speed Guard

Greek symbol

φ	Maintenance factor
ε	Receiver surface emissivity (−)
η	efficiency
σ	Stefan-Boltzmann constant ($W/m^2\ K^4$)

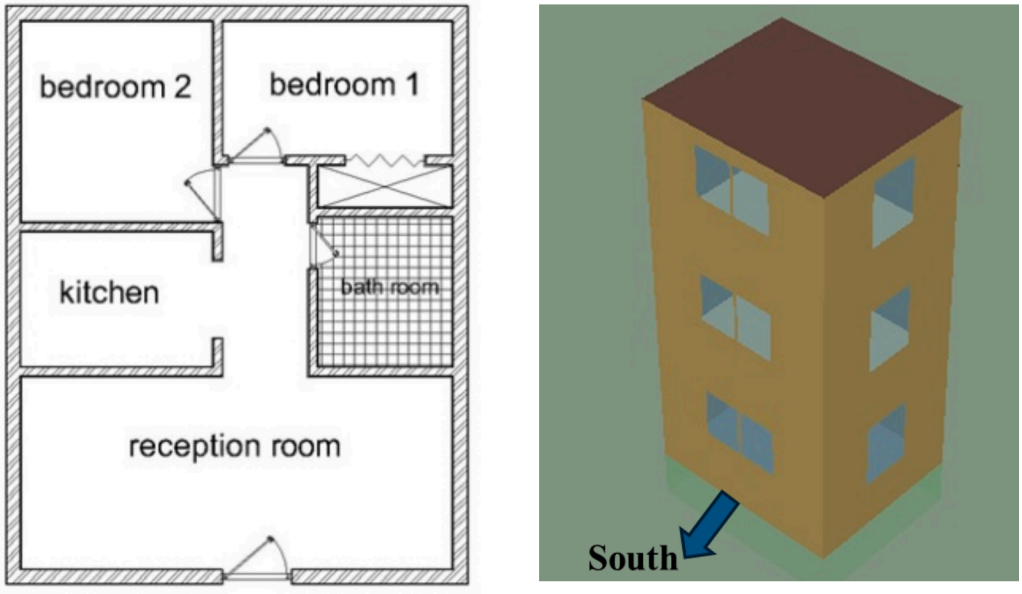

Fig. 1. Proposed Building.

The literature highlights utilizing renewable energy can meet rising energy demands while addressing global warming, as these alternatives are becoming increasingly accessible and cost-effective due to technological advancements and widespread adoption [16–19]. In particular, recent studies have focused on advanced approaches integrating renewable energy into ZEB for residential purposes, including heating and cooling- often identified as key obstacles to achieving fully zero-energy residential solutions [20,21]. Such efforts align with the growing need for cost-effective and energy-efficient solutions in building design [22]. Among various renewable options, wind and solar power stand out for their widespread availability, scalability, and suitability for both small-scale and large-scale implementations, making them particularly attractive for residential use [23,24]. These systems can also be designed to be grid-friendly, promoting smooth integration with existing infrastructure, enhancing overall stability and reliability [25]. Moreover, the development of hybrid wind and solar systems, combined with other renewable sources like geothermal that ensure continuous power generation, can remarkably improve system performance [23,26,27]. Innovations such as incorporating Reverse Osmosis (RO) desalination with renewable energy systems, as seen in

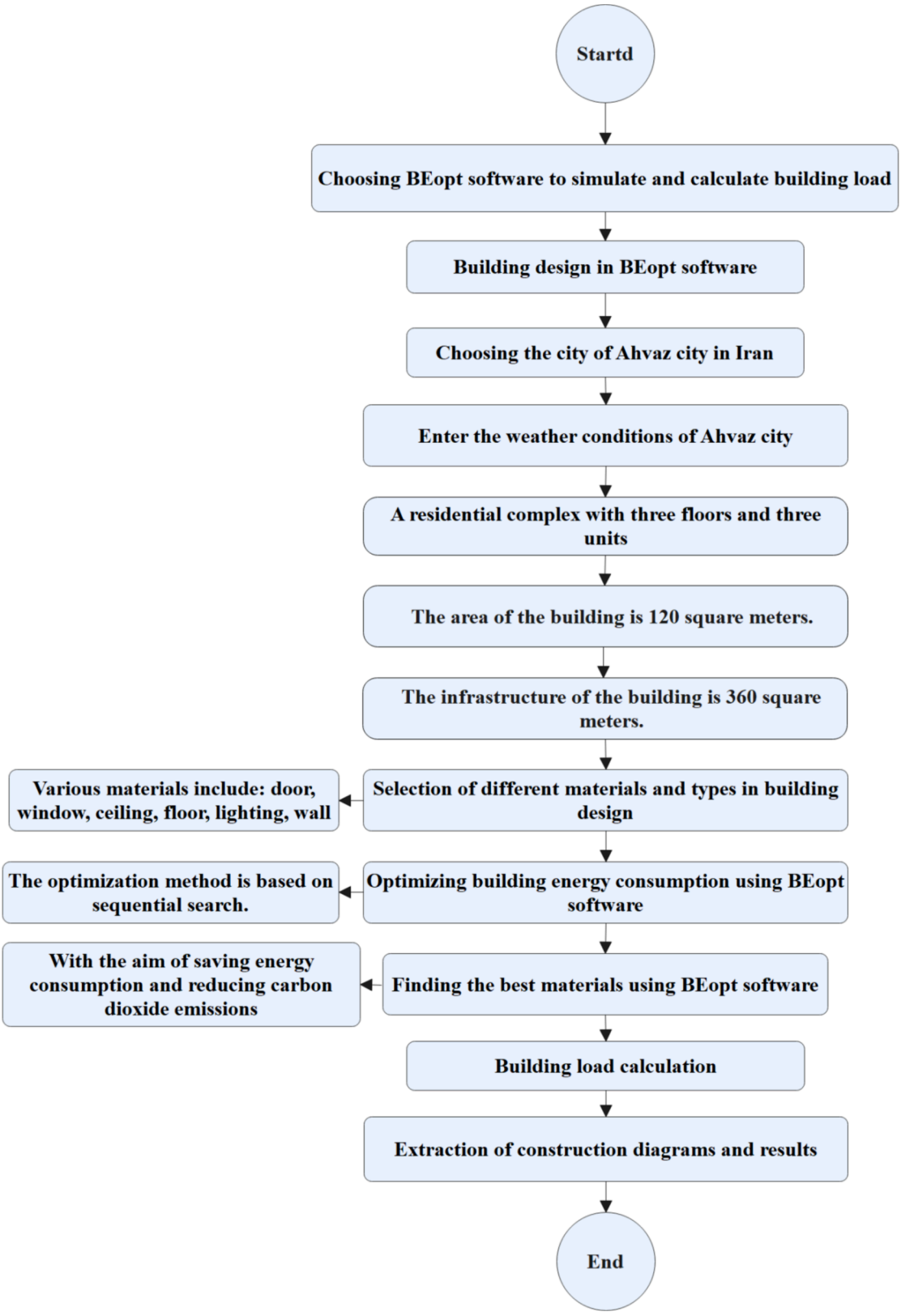

Fig. 2. Process for Analyzing Building's Power, Heating, and Cooling Needs.

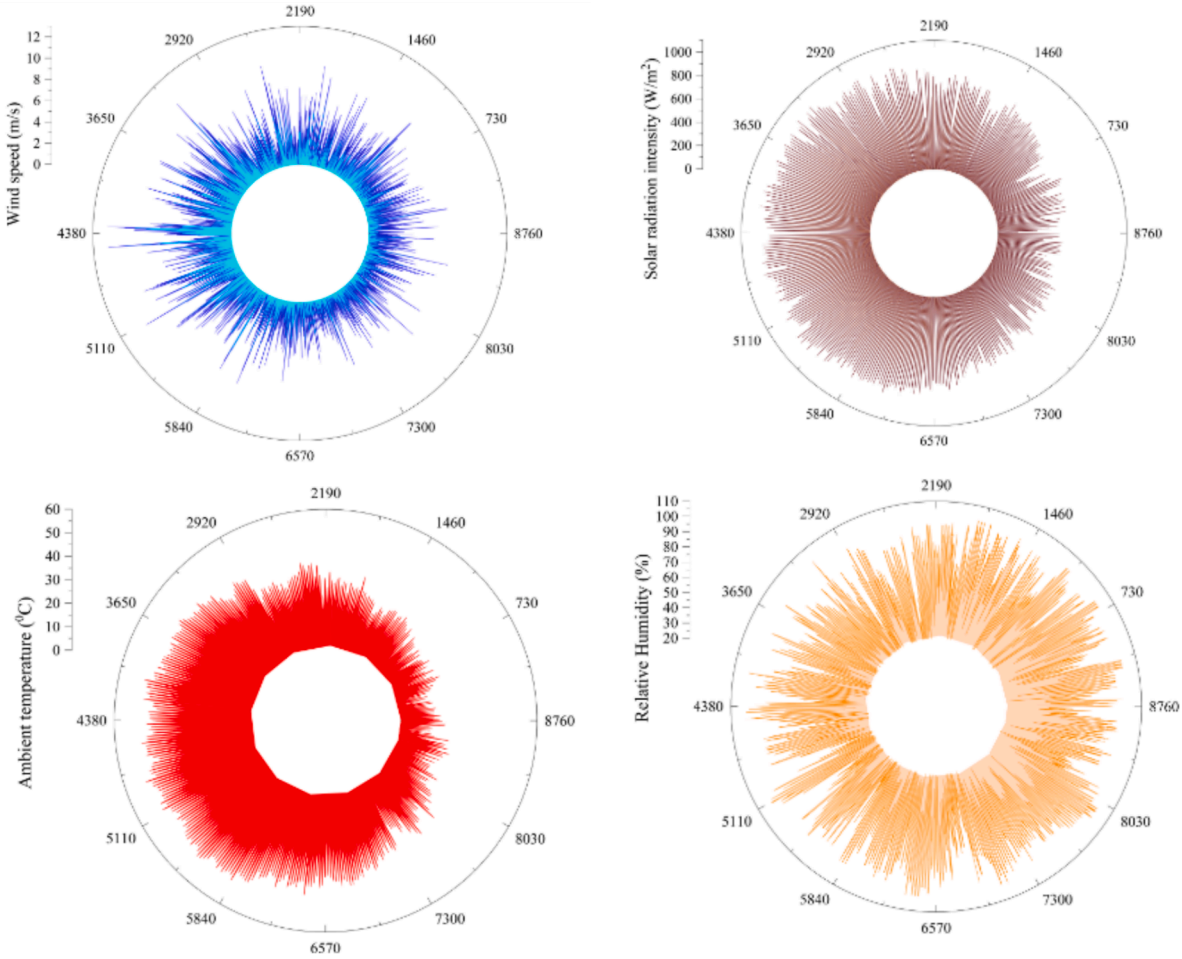

Fig. 3. Hourly Weather Parameters in the Case Study (31.3200°N, 48.6692°E) [56].

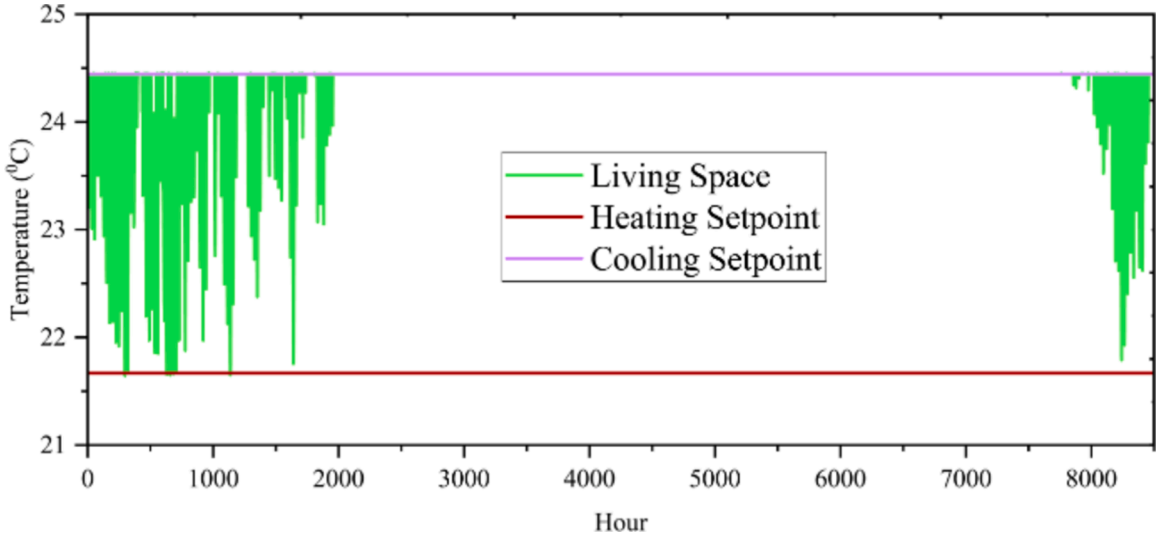

Fig. 4. Yearly Fluctuations in Living Space Temperatures in Ahvaz (31.3200°N, 48.6692°E).

hydropower-wind combinations, highlight the expanding scope of multi-resource energy systems [28]. These integrated systems not only deliver electricity but also provide vital resources like freshwater, illustrating their broader role in meeting global sustainability objectives.

Previous studies have proposed and conducted techno-economic evaluations of various innovative hybrid solar-wind systems, supplemented by another renewable source that provides continuous power generation, demonstrating their potential to optimize energy production and efficiency [29,30]. For example, Assareh et al. [27] integrated solar and geothermal energies with hydrogen production, substantially improving overall energy performance efficiency. In another study, Assareh et al. [31] examined the hybrid systems' role in

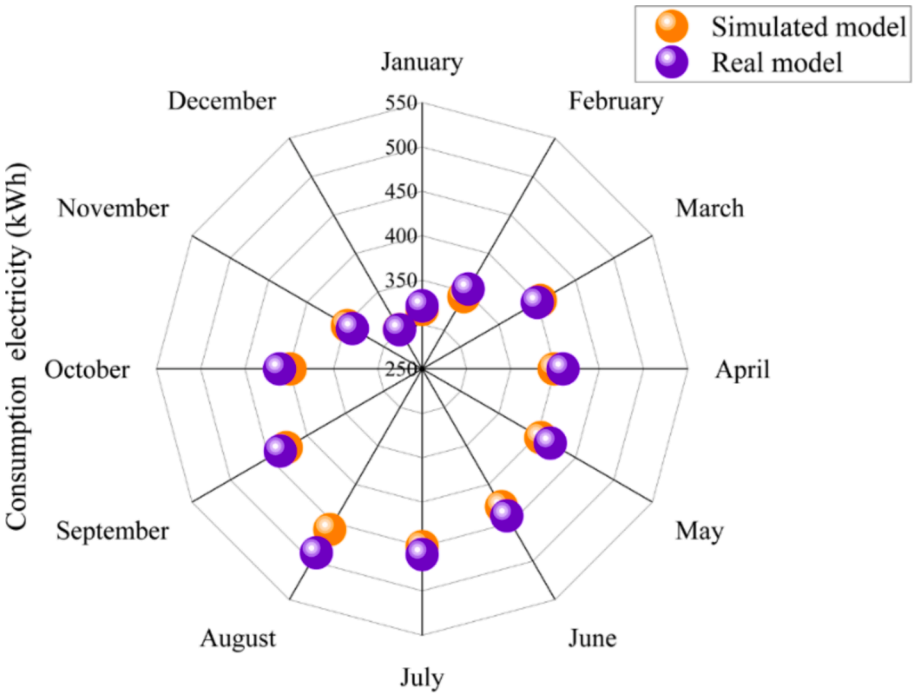

Fig. 5. Validation: Actual vs. BEopt-modeled Electricity Usage.

Table 1
Comparative Error Between Actual and Predicted Electricity Usage.

Month	Actual Consumption (kWh)	Predicted Consumption (kWh)	Error (%)
January	317.00	321.00	1.26
February	344.00	354.00	2.91
March	404.00	405.00	0.25
April	398.99	409.00	2.51
May	404.62	417.00	3.06
June	429.00	441.00	2.80
July	450.00	459.00	2.00
August	458.81	489.00	6.58
September	427.06	435.00	1.86
October	399.07	411.00	2.99
November	347.60	349.00	0.40
December	301.22	302.00	0.26

Table 2
Comparison of Energy Consumption, CO_2 Emissions, and Optimization Scenarios.

Option	Electricity	CO_2 emission	Cooling bar	Heating bar
Optimal	12,145	6970	6023	0.94
Min Cost	9845	6047	4811	0.864
Max Saving	10,123	6361	5291	0.913

achieving sustainable goals by conducting a techno-economic investigation of a multi-source renewable system for combined energy applications (i.e., M−RCCHP). This study demonstrated the capability of fuel cells, photovoltaic panels, and wind turbines as primary contributors to electricity production. The literature also shows that researchers have integrated other energy sources, such as gas turbines [32], geothermal [33,34], hydrogen [35], biomass [36], and biogas [37] with hybrid solar and wind systems to cogenerate electricity and freshwater employing desalination methods like RO [38–40], making them highly suitable for different building functions [41], including residential buildings [42,43].

Building on these findings, the challenge of achieving ZEB status in residential buildings, particularly in regions with extreme climates, presents unique obstacles [44,45]. High cooling loads, reliance on traditional sources and the requirement for a steady energy supply make it especially challenging to achieve zero-energy status in homes, particularly in cooling-dominant climates where cooling demands are substantial and traditional solutions often fall short of sustainability goals [46]. However, recent advancements in energy systems, such as the integration of Modified Steam Rankine Cycles (MSRC) with hybrid solar and wind co-generation systems, have shown promise in addressing these challenges [47,48]. Furthermore, using advanced tools like Building Energy Optimization (BEopt) simulations and the evolutionary computation algorithm and statistical approaches, e.g., Response Surface Method (RSM), has been crucial in fine-tuning these systems for maximum efficiency, ensuring that they can operate effectively even under peak load conditions [43,49–54]. As a result, these integrated approaches can assist in achieving net-zero energy in houses, demonstrating that with the right technology and design strategies, we can overcome the significant challenges posed by extreme climates.

This study addresses a critical question: how can a hybrid solar-wind co-generation system's performance be optimized to generate enough energy for residential demand (heating, cooling, and freshwater), particularly in hot severe climates? It offers innovations, such as using pitch angle control in wind turbines and integrating with technologies, such as MSRC and RO desalination. BEopt simulations and RSM are employed to optimize system performance across multiple variables. In this paper, Section 2 analyzes the residential building's structure and energy needs. Section 3 explores the proposed solar-wind co-generation system, detailing its components and optimization using RSM. Section 4 presents the system's validation, optimization results, and the impact of environmental factors on performance. Finally, Section 5 concludes the study, highlighting key findings and offering recommendations for future research.

2. Building structure and analysis

This study involved designing a 3-unit apartment, with each unit measuring 120 m2, located in Ahvaz's subtropical hot desert climate, characterized by prolonged, hot summers and mild winters, as

(a)

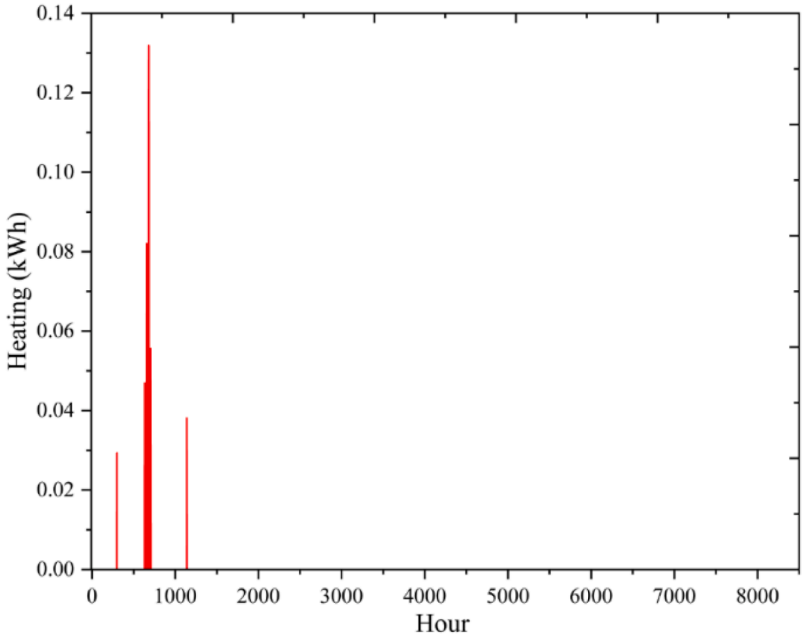

(b)

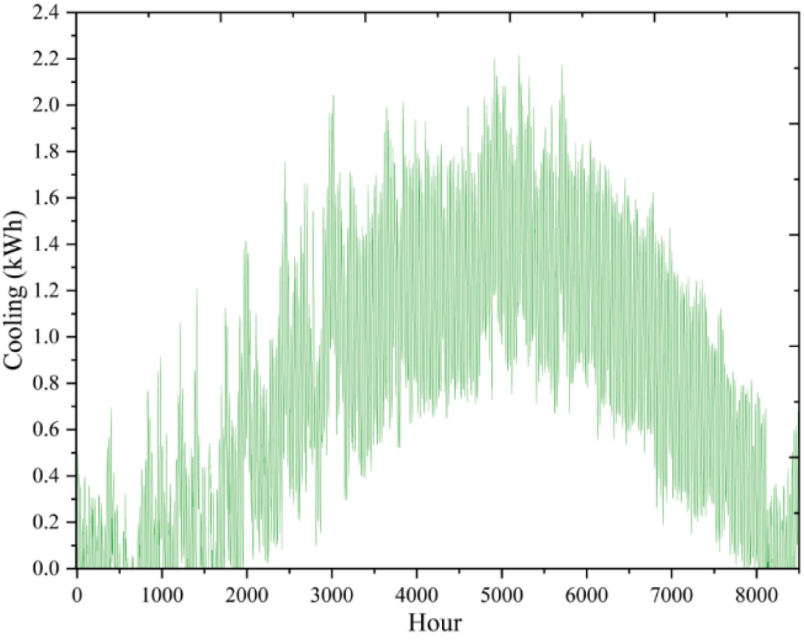

(c)

Fig. 6. Hourly Energy Patterns: (a) Heating Load, (b) Cooling Load, and (c) Energy Consumption.

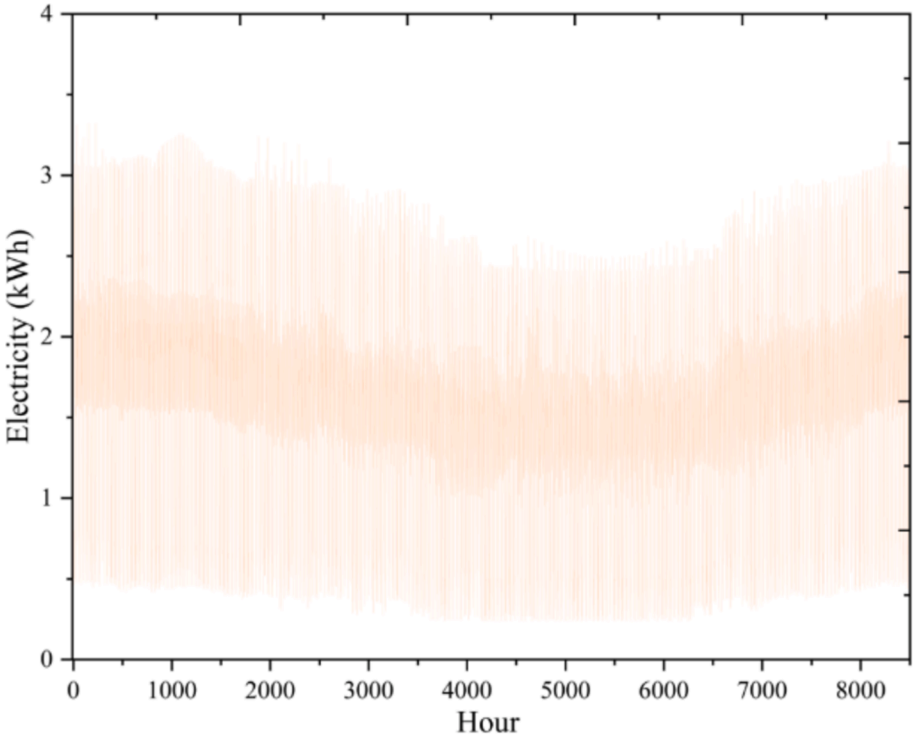

Fig. 6. (*continued*).

illustrated in Fig. 1. The aim was to assess the annual power output, as well as the heating and cooling requirements for the entire building, which houses a total of 15 occupants, using BEopt software [55]. BEopt was chosen for its ability to optimize residential energy performance while integrating renewable systems, which aligns with the study's goals for ZEB design. Its parametric optimization features identify cost-effective strategies, and its integration of localized climate data ensures accurate simulations under Ahvaz's extreme conditions. BEopt's also focus on residential modeling and user-friendly interface make it a reliable choice compared to other tools like EnergyPlus or TRNSYS, which cater to broader applications but lack specific residential optimization capabilities.

The primary objective was to develop an integrated co-generation system capable of meeting the building's energy demands. BEopt facilitated detailed simulation-based analysis and design optimization, considering factors such as building size, architecture, occupancy, location, and financial parameters. BEopt is used to evaluate both new construction and retrofit scenarios, identifying cost-effective solutions to enhance the building's overall energy efficiency.

The diagram in Fig. 2 outlines the step-by-step process used to analyze the residential building. It includes the design and assessment of the power, heating, and cooling needs that are crucial for the building's structure.

The optimal design of the residential building, oriented to face north, involved selecting appropriate sizes for doors and windows, choosing suitable materials for walls and ceilings, and using Phase Change Materials (PCM) within the building envelope. A thorough optimization analysis was conducted to minimize the building's energy usage. To handle the large volume of data and analyses, a powerful computer system was utilized. The optimization process involved 54 simulation runs and took about 10 h and 25 min to complete. The study looked at hourly changes in key weather and environmental conditions in Ahvaz city over a year (8,760 h), including Air temperature (T_0), Wind speed (WS), Solar radiation intensity (SRI), Relative humidity (RH), and Dew Point (DP).

These environmental factors significantly influence building power consumption and generation patterns. Fig. 3 shows the hourly fluctuations of these parameters throughout the year in Ahvaz. The highest wind speeds, solar radiation, and ambient temperatures occur in June and July, which are the hottest months of the year. In contrast, January, the most humid month, represents the cooler season. Understanding these dynamic weather patterns significantly influences the design and optimization of hybrid renewable energy systems in the region. For example, high solar radiation and temperatures in summer increase the potential for solar energy harvesting, while elevated wind speeds improve wind turbine performance. However, the concurrent rise in ambient temperatures can reduce the efficiency of photovoltaic systems, necessitating strategies such as improved ventilation and thermal management to maintain performance.

Conversely, high relative humidity during winter challenges hydrogen storage and production systems, as it affects electrolysis efficiency and material durability. The observed fluctuations highlight the importance of integrating adaptive strategies, such as advanced control algorithms and hybrid energy systems, to capitalize on seasonal variations in renewable energy resources while mitigating operational inefficiencies. Optimizing these systems based on such dynamic weather conditions enhances energy generation and ensures resilience and sustainability in extreme climates like Ahvaz.

Fig. 4 illustrates the fluctuations in living space temperatures throughout the year in Ahvaz. This data highlights the importance of maintaining an ideal temperature range between 21.5 °C (70°F) and 24.5 °C (76°F) to ensure an optimal and comfortable indoor climate for residents. The setpoint temperature for cooling and heating is the normal limit for maintaining these ideal temperature conditions. The temperature variations depicted emphasize the strong influence of the local climate on thermal behavior. Given outdoor temperatures often exceed the comfortable range for indoor living spaces, it is crucial to optimize the building's design and energy systems to effectively regulate the indoor environment and maintain the target temperature band (21.5 °C–24.5 °C). In this figure, the green lines represent periods when the living space remains within the comfort zone without any heating or cooling, as temperatures stay between the setpoints. The analysis

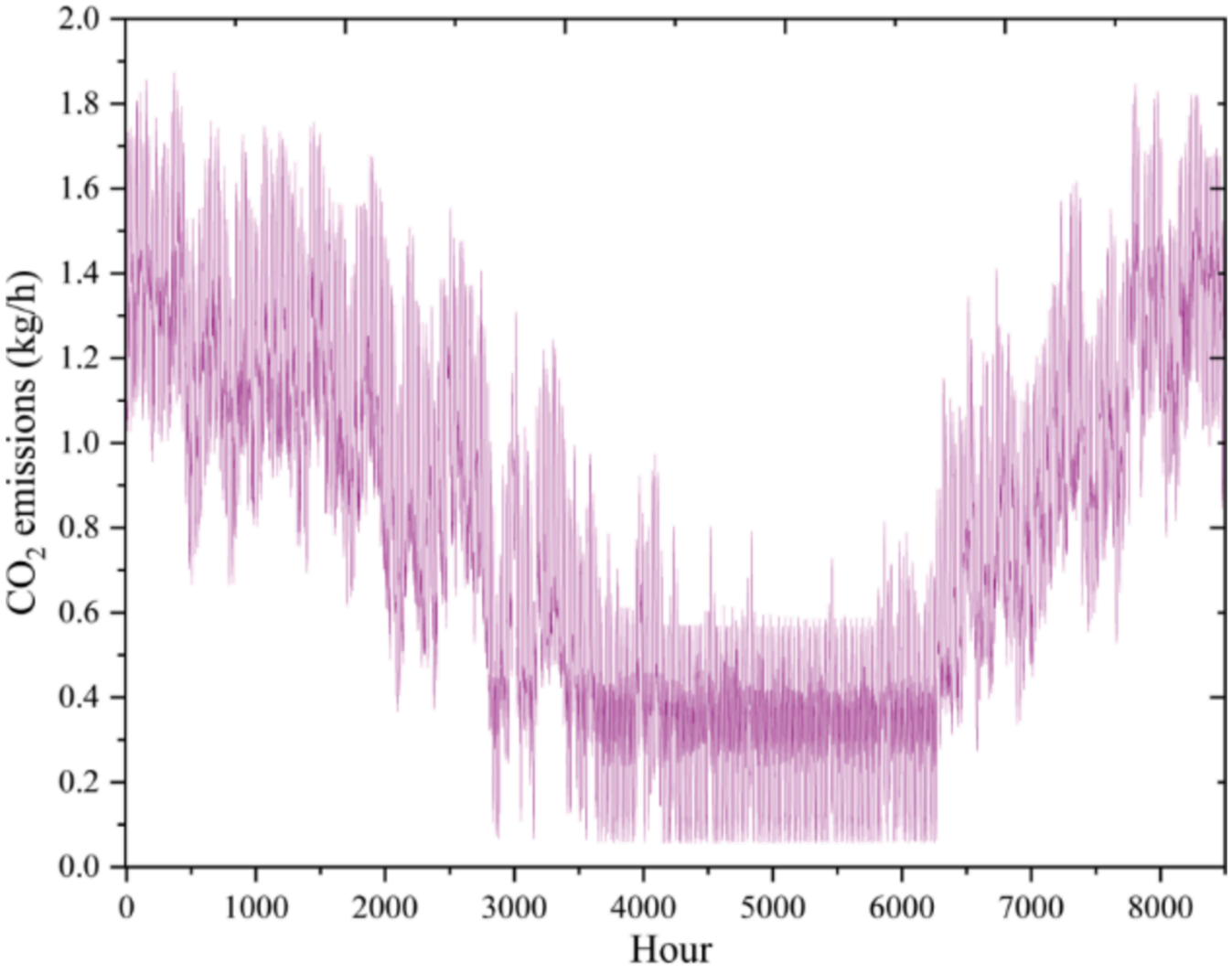

Fig. 7. Hourly CO_2 Emissions.

indicates that heating and cooling are not required from December to mid-March.

This optimization may involve strategies such as:

- Enhancing the building envelope's thermal insulation and airtightness to minimize heat gains and losses.
- Incorporating passive cooling techniques, such as natural ventilation and shading, to reduce the reliance on mechanical cooling
- Deploying efficient HVAC systems, potentially leveraging renewable energy sources like solar or geothermal, to provide heating and cooling as needed
- Implementing intelligent control systems to dynamically adjust the building's energy systems based on occupancy and environmental conditions

By carefully designing and operating the building to maintain the target temperature range, occupants can enjoy a comfortable and healthy living space, reducing both energy use and carbon footprint. The insights provided by Fig. 4 underscore the importance of considering the local climate and its impact on building performance during the design and optimization process. This knowledge can help create more sustainable, energy-efficient structures in Ahvaz and similar hot climates.

2.1. Validating electricity consumption in Ahvaz residential units

Fig. 5 compares the actual electricity consumption of a 120-square-meter residential unit on the ground floor in Ahvaz and the consumption predicted by the BEopt software model. In addition to this visual representation, a detailed quantitative analysis of the discrepancies between actual and predicted electricity consumption is presented in Table 1.

The data indicates that the actual residential unit shows higher electricity usage during the summer and hot seasons, primarily due to the increased use of cooling devices, such as air coolers and split air conditioning systems, to maintain thermal comfort in Ahvaz's hot climate. Conversely, electricity consumption decreases during the colder seasons as the demand for cooling diminishes. In the software-analyzed model, the cooling equipment is simulated as being powered by the national electricity grid, replicating the real conditions in Ahvaz. This approach ensures a more accurate validation of the building's electricity consumption trends over a year. By comparing real-world electricity usage data with the BEopt software model, researchers were able to confirm the accuracy of the simulation tool in predicting the building's energy consumption patterns. This validation process is crucial for developing reliable energy optimization strategies and ensuring the system's effectiveness. The insights gained from this analysis can inform the design and management of energy-efficient residential structures in

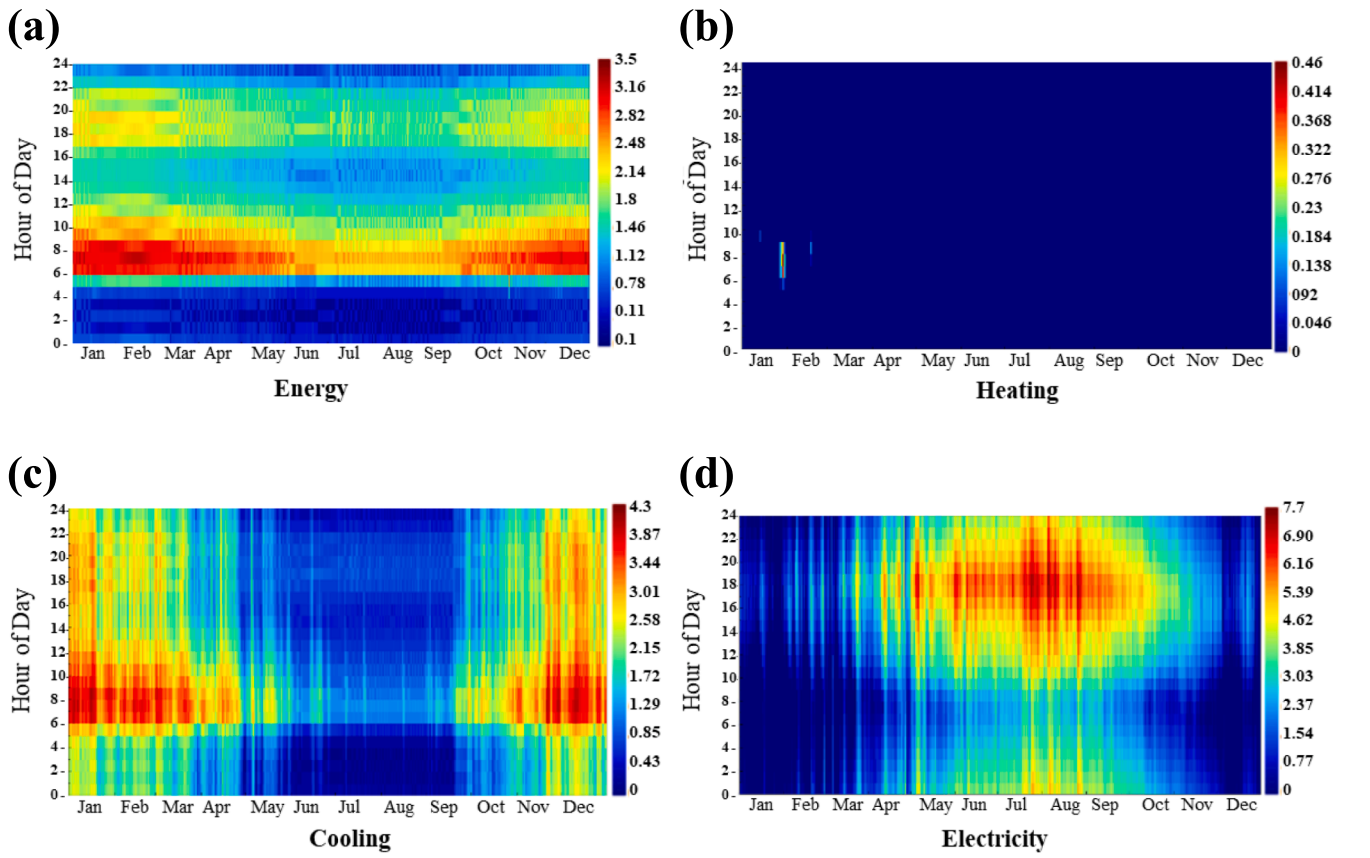

Fig. 8. Thermal Contours (a) Energy, (b) Heating, (c) Cooling, and (d) Electricity Consumption.

Ahvaz, considering the region's unique climate and the cooling needs of its occupants. This knowledge can support the development of more sustainable and cost-effective zero-energy building solutions tailored to the local context.

2.2. *Optimization of building structure (optimum results)*

Table 2 summarizes the outcomes of the optimization process conducted via BEopt, targeting improvements in residential building energy consumption, construction cost, and CO_2 emission. The optimization, encompassing 54 iterations over 10 h and 25 min, considered various factors such as local weather conditions and the specific materials used in construction.

Three primary scenarios were evaluated:

- **Optimal State:** This scenario represents the ideal balance of electricity consumption, heating, and cooling, aiming to save energy, reduce costs, and minimize environmental impact.
- **Energy-Saving Mode:** This scenario prioritizes energy conservation above all else.
- **Cost-Reduction Mode:** This scenario focuses on minimizing construction expenses.

For this study, the optimal mode was selected, as it offers a comprehensive approach to optimizing energy usage, cost-effectiveness, and environmental sustainability simultaneously.

The first scenario, labeled as the optimal state, represents the ideal balance between electricity consumption, heating, and cooling, aiming to save energy, reduce costs, and minimize environmental impact simultaneously. The energy-saving mode prioritizes conservation above all else, while the cost-reduction scenario focuses on minimizing construction expenses. For this study, the optimal mode was selected, as it offers the most comprehensive approach to optimizing energy usage, cost-effectiveness, and environmental sustainability.

By optimizing the selection of building materials, consumables, and structural design, the best possible energy performance can be achieved for a residential building project. The proposed system's performance is illustrated through its annual energy patterns. The hourly heating load consumption (Fig. 6a) reveals minimal demand, ranging between 0 and 0.14 kWh throughout the year, reflecting the warm climatic conditions of Ahvaz City, where strong solar radiation and consistently high ambient temperatures reduce the need for heating. Conversely, the hourly cooling load consumption (Fig. 6b) demonstrates a substantial demand, fluctuating between 0 and 2.4 kWh annually, driven by persistently high temperatures that necessitate significant cooling to maintain indoor comfort. This highlights the importance of advanced cooling technologies and thermal insulation to improve energy efficiency in warm climates. Fig. 6c shows the hourly electricity consumption for the proposed building, highlighting the reliance on active systems to meet cooling demands. Optimizing hybrid renewable energy systems, such as the integration of wind and solar power, is crucial for sustainably addressing these energy requirements while ensuring optimal building performance in such extreme conditions.

Fig. 7 displays the annual reduction in CO_2 emissions because of optimizing the residential building's energy usage. This data shows a correlation between the reduction in electricity consumption and a subsequent decrease in carbon dioxide emissions. This highlights the significant contribution of electricity consumption to carbon dioxide emissions, emphasizing the importance of reducing energy use to effectively limit CO_2 emissions.

The CO_2 emissions avoided were calculated by assuming that the electricity displaced by the renewable energy system would otherwise have been generated by fossil fuel power plants, emitting 0.204 tons of CO_2 per MWh. Using this emission factor, the total emissions avoided

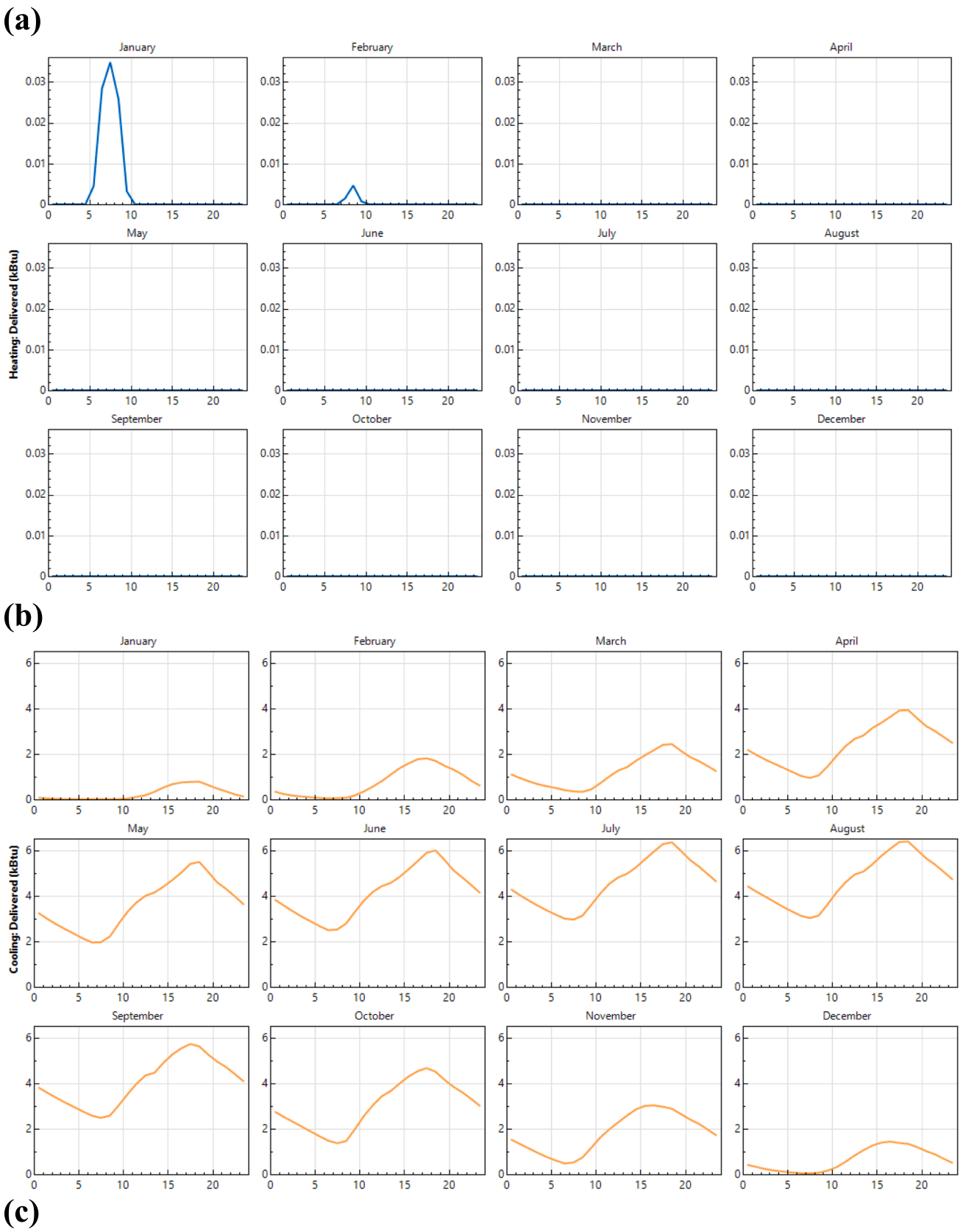

Fig. 9. Monthly Energy Demand Profile (a) Heating, (b) Cooling, and (c) Power.

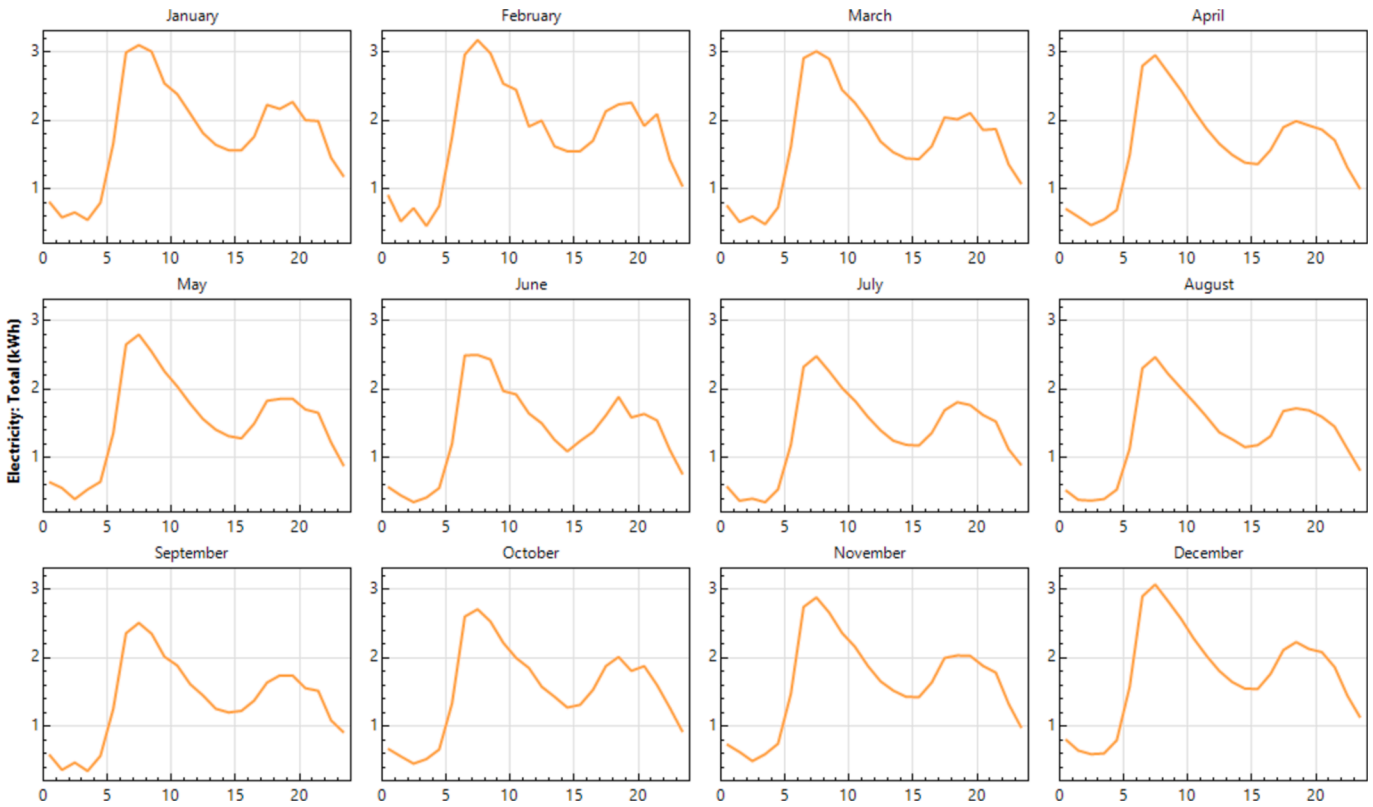

Fig. 9. (*continued*).

were determined as the product of annual electricity generation by the system and the emission factor. For the annual electricity generation of 6,541.564 MWh, the reduced emissions are 1,334.47 tons of CO_2 annually. This calculation assumes constant efficiency and emission rates for the baseline energy source, consistent with regional energy profiles.

Fig. 8 portrays the thermal contours illustrating the hourly energy demand and distribution within the residential building. These contours represent the calculated energy consumption, heating load, cooling demand, and power usage required by the building across various seasons, considering the materials used in its construction. These contours capture the variations in energy consumption for residential purposes over months of the year, influenced by the environmental conditions affecting the residential building.

Fig. 9 illustrates the monthly energy demand profiles for the optimized structure. Fig. 9 (a) shows the heating demand, primarily concentrated in January and February, reflecting the colder months. Fig. 9 (b) depicts the cooling demand, with significant peaks observed in July and August during the summer season, driven by persistently high temperatures that necessitate substantial cooling to maintain indoor comfort. This highlights the importance of integrating advanced cooling systems and passive design strategies to manage peak loads effectively. Fig. 9 (c) presents the monthly electricity consumption profile, which ranges between 0.2 and 3.2 kWh, highlighting the energy requirements of the optimized building throughout the year. These patterns emphasize the need for optimizing renewable energy systems, such as wind and solar integration, to sustainably meet the building's fluctuating energy demands while ensuring efficient performance in extreme climatic conditions.

Fig. 10 displays the impact or sensitivity of various environmental parameters such as T_0, SRI, WS, and RH on the heating consumption of the building over one year in Ahvaz. This visual representation helps to understand how changes in these factors influence the building's heating needs over time. The heating demand ranges between 0 and 0.6 kWh, reflecting the warm climatic conditions that minimize heating requirements. WS influences heating demand by affecting the rate of heat loss through infiltration and natural ventilation. RH also impacts heating by modulating perceived indoor comfort and latent heat transfer. SRI and ambient temperature T0 reduce heating demand by naturally warming indoor spaces, with their effects, like wind speed, ranging between 0 and 0.5 kWh. These insights validate the BEopt simulation outputs by confirming the expected relationships between climatic conditions and heating demand. The trends observed in this figure ensure alignment between simulation assumptions and real-world behavior, enhancing the reliability of the results.

Fig. 11 illustrates the sensitivity of cooling demand to variations in environmental factors like WS, RH, SRI, and T_0 annually. This visualization helps in understanding the sensitivity of cooling needs to fluctuations in these environmental parameters across different seasons. WS (0–14 m/s) indirectly affects cooling demand by influencing ventilation and heat exchange, while higher RH (0–100 %) increases cooling requirements due to the need for dehumidification. SRI intensities, reaching up to 1000 W/m^2, contribute to heat gains in indoor spaces, emphasizing the importance of passive measures such as shading and reflective materials. Lastly, cooling demand rises significantly as T0 ranges from 7 °C to 32 °C, demonstrating the strong correlation between higher temperatures and increased cooling needs.

Fig. 12 demonstrates the nuanced influence of distinct environmental parameters, WS, RH, SRI, and T_0 on residential electricity usage, which ranges from 0.2 to 3.5 kWh throughout the year in Ahvaz.

Fig. 13 illustrates the energy consumption costs, accrued energy savings, and corresponding reductions in CO_2 emissions at various stages of the building's optimization process. Initially, the data points show zero energy savings, representing the baseline performance before optimization. As optimization progresses, energy savings increase, correlating with reduced energy consumption costs and significant CO_2 emissions reductions. This progression reflects the impact of implementing energy-efficient design strategies, such as improved thermal

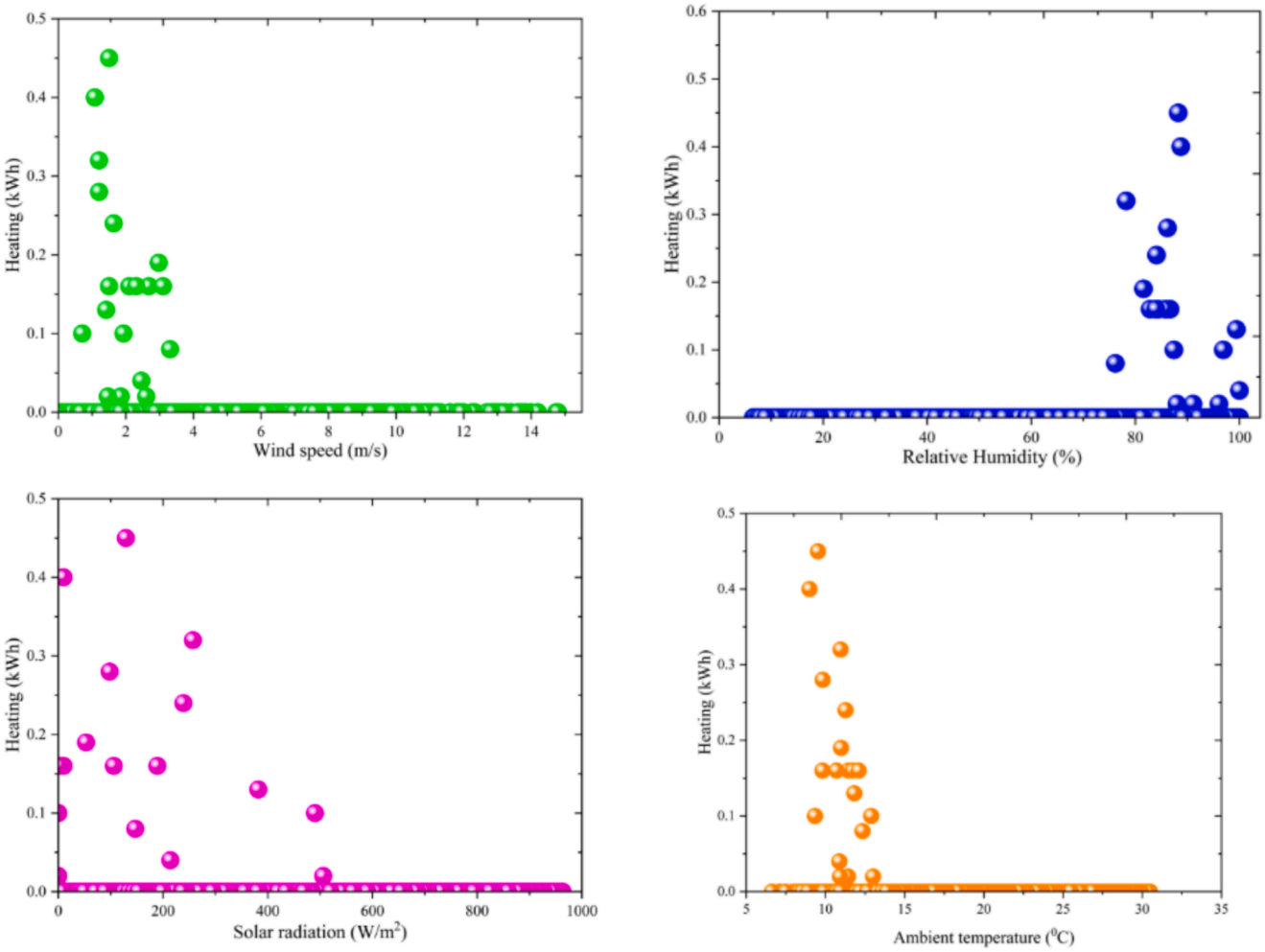

Fig. 10. Influence of Weather Parameters on Heating Load Distribution.

insulation, enhanced glazing, and optimized HVAC systems, which collectively minimize energy demand. The final point highlights the most significant energy savings achieved, demonstrating the effectiveness of the optimization process in reducing operational costs and environmental impacts. These results validate the role of adopted energy-efficient measures in achieving sustainable and economically viable building performance while contributing to climate change mitigation.

Table 3 presents optimal points, categorized alphabetically in the Pareto chart, each reflecting one of three main objectives: saving energy, lowering CO_2 emissions, and cutting costs. The building achieves an annual energy savings rate of 0.34 %, equating to $1,483.57 in annual energy-related cost savings. These results correspond to a site energy savings of 41.97 kWh annually, reflecting the building's improved energy efficiency. The Net Present Value (NPV) of the implemented optimization measures is calculated at $10,575.24, while the life cycle cost amounts to $61,543.54, demonstrating the economic viability of the strategies. The CO_2 savings of 5.67 tons per year align with the reduced reliance on energy-intensive cooling systems, emphasizing the effectiveness of the optimization process in lowering operational emissions. These quantified outcomes validate the balance between energy efficiency, cost-effectiveness, and environmental impact, highlighting the importance of tailored design measures in achieving sustainable building performance in extreme climates.

3. Analysis of the co-generation system (utilization energy)

The main objective is to develop a solar-integrated, multi-renewable energy generation system to power a 3-story residential building in Ahvaz. Each floor houses a single unit, and the system is designed to supply the building's power, cooling, and heating demands by harnessing the area's renewable energy potential, with the ultimate goal of achieving a zero-energy building.

The investigation focuses on the specifications of the solar-wind system that will fulfill the residential building's energy demands. This research evaluates the effect of changes in SRI, WS, and T_0 on the optimal performance. Fig. 14 illustrates the comprehensive flow of this research, highlighting the progression from initial simulations to the proposed energy solutions.

Initial simulations modeled the residential building in accordance with Ahvaz's environmental conditions. A diversified solar energy system was subsequently proposed to fulfill the building's energy requirements. Given Ahvaz's hot climate and abundant solar potential, the study found that the heating load is significantly lower than the cooling load, leading to high air temperatures year-round. Furthermore, the study thoroughly explores the ZEB concept through the integration of renewable energy solutions to meet the unique energy demands of residential structures.

3.1. Cogeneration system explanation

Fig. 15 illustrates the layout of the suggested co-generation scheme,

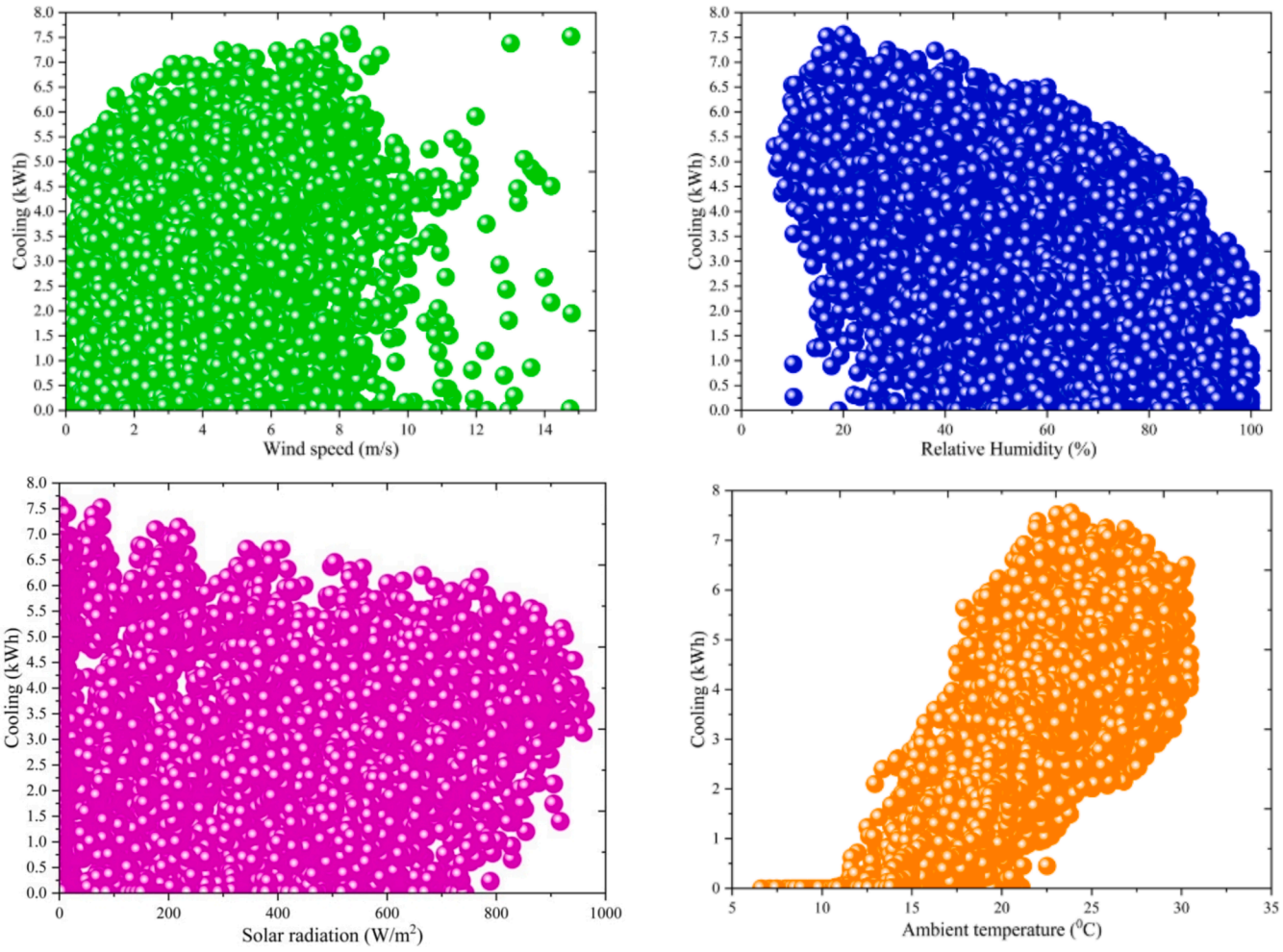

Fig. 11. Effects of Weather Parameters – Load distribution.

featuring RO for desalinating brackish water and a solar unit as the main energy source, and an MSRC. Key components are heliostats or solar concentrators, a Rankine steam turbine, a cooling tower, along with molten salt thermal storage integrated with the RO unit. The system outputs consist of green electricity, cooling, heating, and freshwater, all designed to reduce environmental pollution.

The energy generation process begins with heliostats absorbing solar radiation and directing it to a receiver system, where the solar heat is channeled to a turbine to drive electricity generation. The heliostats concentrate sunlight onto a central receiver, generating high temperatures that power the turbine via the working fluid, functioning as a central receiver thermal power plant. A wind turbine is integrated into the system to further enhance power generation, with performance optimized by controlling the turbine's pitch angle. The evaporator, a critical component, operates efficiently depending on factors such as fluid characteristics, surface properties, pipe types, and temperature differentials. In operation, saturated steam exits the evaporator and enters the superheater, driving the MSRC turbine for electricity production. At this stage, the fluid, now at lower pressure and temperature, flows into the recuperator (preheater), where its heat output is used for residential heating. Following reheating in the evaporator to address the cooling requirements of residential buildings, the fluid is cooled and recirculated within the system, eventually re-entering the pump to complete the cycle.

Fig. 15 illustrates the solar component's performance based on a single efficiency assumption, simplifying the analysis and providing a preliminary evaluation of system feasibility. This approach demonstrates the potential benefits of the co-generation system under ideal conditions, such as achieving energy surplus and reducing carbon emissions. While the analysis focuses on system-level feasibility, future studies could incorporate dynamic efficiency models to capture variations in solar performance due to environmental factors like temperature and irradiance.

3.2. Pitch angle control (wind turbine)

This study examines the National Renewable Energy Laboratory (NREL)' wind turbine model. This turbine is characterized as a horizontal axis, upwind, offshore, variable speed, and variable pitch type. The specific attributes of this turbine are detailed in [40], and these specifications enable the creation of a mathematical model to represent the turbine's functionality. Key specifications of the turbine are shown in Table 4.

The NREL 5 MW wind turbine model's primary components consist of the aerodynamic system, drivetrain, generator, and propeller start mechanism.

3.2.1. Aerodynamic system model

The wind turbine's aerodynamic power output can be characterized by Eq (1):

$$P_a = \frac{1}{2}\rho\pi R^2 C_p(\lambda,\beta)v^3 \quad (1)$$

where ρ and ν are air density and wind speed respectively. P_a is also

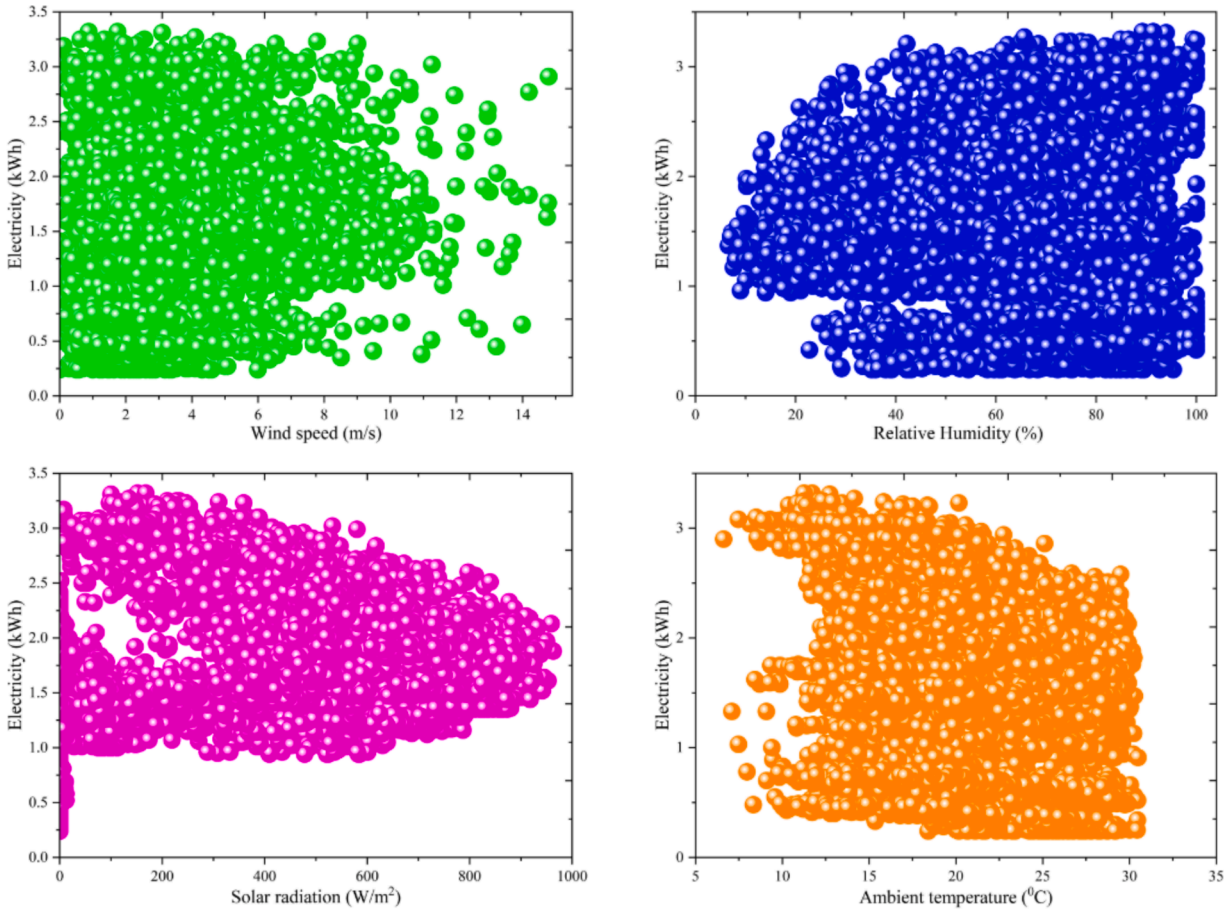

Fig.12. Effects of Weather on Electricity Consumption & Load Distribution.

called mechanical power, and it is obtained because of the wind driving the rotor, causing it to rotate.

The power coefficient C_p is influenced by the pitch angle β and the tip speed ratio λ (TSR). The tip speed ratio λ is defined by Eq. (2):

$$\lambda = \frac{\omega_r R}{v} \tag{2}$$

where ω_r is the speed of the rotor.

As illustrated in Fig. 16, this method involves minimizing the discrepancy between the generator's actual and nominal speeds using the optimal Proportional-Integral (PI) controller. The PI generates the appropriate pitch control signal interval β_{ref} in its output. β_{ref} is obtained from Eq. (3):

$$\beta_{ref}(t) = K_p e(t) + K_i \int_0^t e(\tau) d\tau \tag{3}$$

where K_p and K_i represent the PI controller's proportional and integral gain parameters, respectively, and $e(t)$ can be expressed as follows based on Eq. (4):

$$e(t) = \omega_{g,n} - \omega_g(t) \tag{4}$$

where $\omega_{g,n}$ and $\omega_g(t)$ are the generator's nominal and actual speeds.

According to Equation (4), the proposed cumulative pitch controller determines the appropriate reference pitch angle, represented as β_ref, fine-tuning the pitch angle β. Adjusting β affects ω_r, and subsequently ω_g. When functioning correctly, the controller maintains ω_g, near ω_{gn}, while also keeping T_g nearly its rated values.

3.2.2. *Wind turbine simulation results*

In this section, the NREL wind turbine is employed to assess the performance of using the pitch angle controller. To assess the effectiveness, a comparison was made with a typical PI controller. Fig. 17 illustrates the typical configuration of a PI pitch controller. The gain values are $K_p = -1.03$, $K_i = -19.46$, chosen based on 15 m/s and determined using the FA method.

The wind speed profile depicted in Fig. 18 uses 15 m/s wind speed (average) to facilitate a comparative analysis between the two controllers. This profile is derived from the Kaimal wind model [53].

Fig. 19 illustrates the performance of the proposed controller compared to the conventional Proportional Integral (PI) controller. Fig. 19 (a) shows that the proposed controller achieves smoother and less fluctuating changes in the pitch angle, reducing energy usage by the pitch actuator system; fluctuations are reduced from a range of 0 to 20 (Conventional PI controller) to 0–16 (proposed controller). Fig. 19 (b) demonstrates that both controllers maintain the generator's output power near the nominal value of 5 MW, but the proposed controller exhibits a narrower range of fluctuations, indicating superior power stability. Fig. 19 (c) highlights that the proposed controller maintains the generator speed with smaller fluctuations around the nominal value of 122.9 rad/s, well within the Over Speed Guard (OSG) limit of 160 rad/s, thereby enhancing safety and minimizing the risk of exceeding operational thresholds.

The pitch starter system is an electro-hydraulic mechanism essential for rotating the wind turbine blades along their pitch axis. Its primary function is to mitigate stress during high wind speeds and storms, preventing potential damage to the turbine and enhancing operational safety. It also enables precise adjustment to the generator's power output by altering blade angles. While smaller wind turbines often use

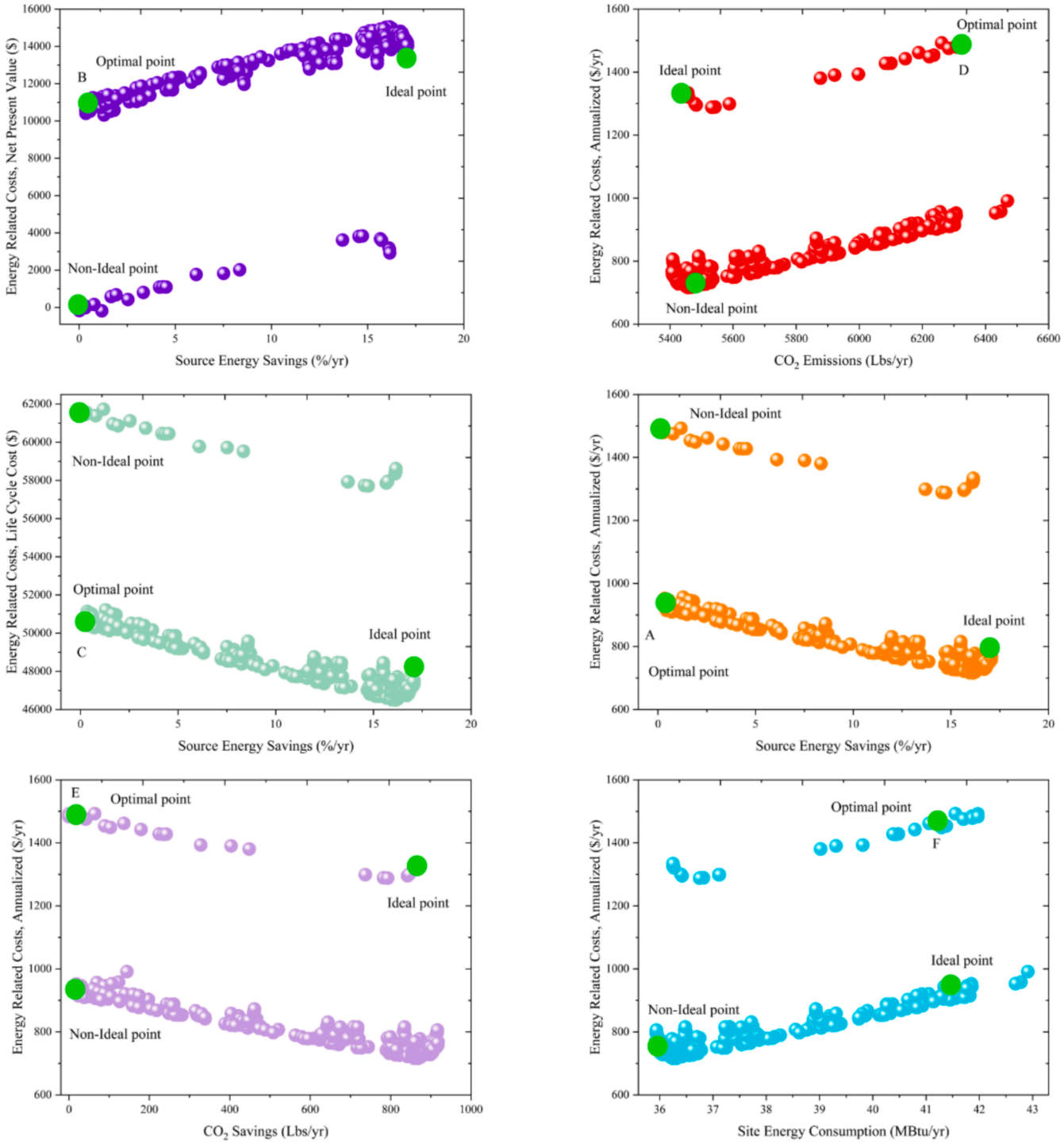

Fig. 13. Annual Energy Cost across Different Optimization Modes.

Table 3
Optimal Parameters for Energy Savings and CO2 Reduction.

Optimal Points	Targets	Value
A	Energy Saving	0.34
	, Annualized	1483.57
B	Source Energy Saving	0.34
	Net Present Value	10575.24
C	Energy Saving	0.34
	Life Cycle Cost	61543.54
	CO_2 Emissions	6325.21
D	, Annualized	1483.57
	CO_2 Savings	5.67
E	Annualized	1483.57
	Site Energy	41.97
F	Source Energy Saving	0.34
	, Annualized	1483.57

fixed rotor blades without rotational capacity, larger, variable-pitch turbines incorporate this system to dynamically adjust blade angles based on commands from the control system, optimizing performance and efficiency under varying wind conditions.

3.2.3. Effect: pitch angle control

Wind turbines generate power that can meet or exceed the nominal output at high wind speeds, especially when these speeds surpass the specified threshold. Managing this excess power is crucial for maintaining stability and preventing undue stress on the turbine system, thereby averting potential damage. One effective strategy for achieving this involves the use of pitch angle control. In wind turbines equipped with variable-pitch functionality, adjusting the blade rotation around their axis alters the blades' angle of attack. This adjustment reduces the blade rotation speed in response to rising wind, thereby stabilizing the turbine's power output around its nominal value. Consequently, this approach effectively prevents power loss and protects the system from excessive stress or strain.

3.3. System equations and analytical framework

The following equations describe the performance of each component in the proposed system:

3.3.1. Solar panels

$$P_{solar} = \eta_{solar} \times A \times G \tag{5}$$

In this equation, P_{solar} is the power output, η_{solar} is the panel efficiency, A is the panel area, and G is the solar irradiance.

3.3.2. Thermal systems (Heating and Cooling)

For calculations of heating and cooling load, the Eqs. (6) and (7) are employed.

$$Q_{heating} = \mathrm{m} \times C_P \times \Delta T \tag{6}$$

$$Q_{cooling} = \mathrm{m} \times h_{fg} + \mathrm{m} \times C_P \times \Delta T \tag{7}$$

Where mmm is the mass flow rate, C_p is the specific heat capacity, ΔT is the temperature difference, and where h_{fg} is the latent heat of vaporization.

3.3.3. Reverse Osmosis (RO) desalination

RO desalination is calculated using Eq. (8):

$$W_{RO} = \frac{P \times Q}{\eta_{pump}} \tag{8}$$

where W_{RO} is the work required, P is the operating pressure, Q is the water flow rate, and η_{pump} is the pump efficiency.

4. System results

This section outlines the key findings from the evaluation of the suggested solar-wind hybrid system, including validation, optimization, and performance metrics under Ahvaz's climatic conditions. The results

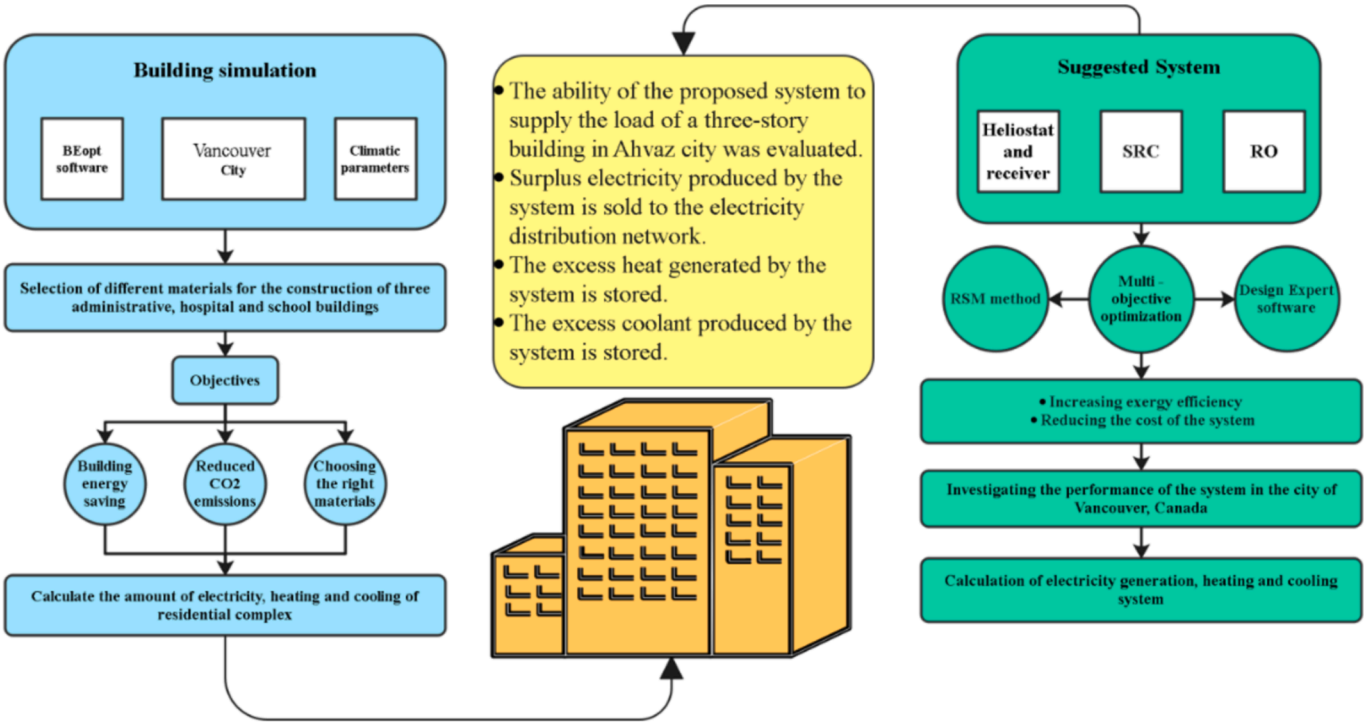

Fig. 14. Overview of the Zero-Energy Building (ZEB) System Design and Process Flow.

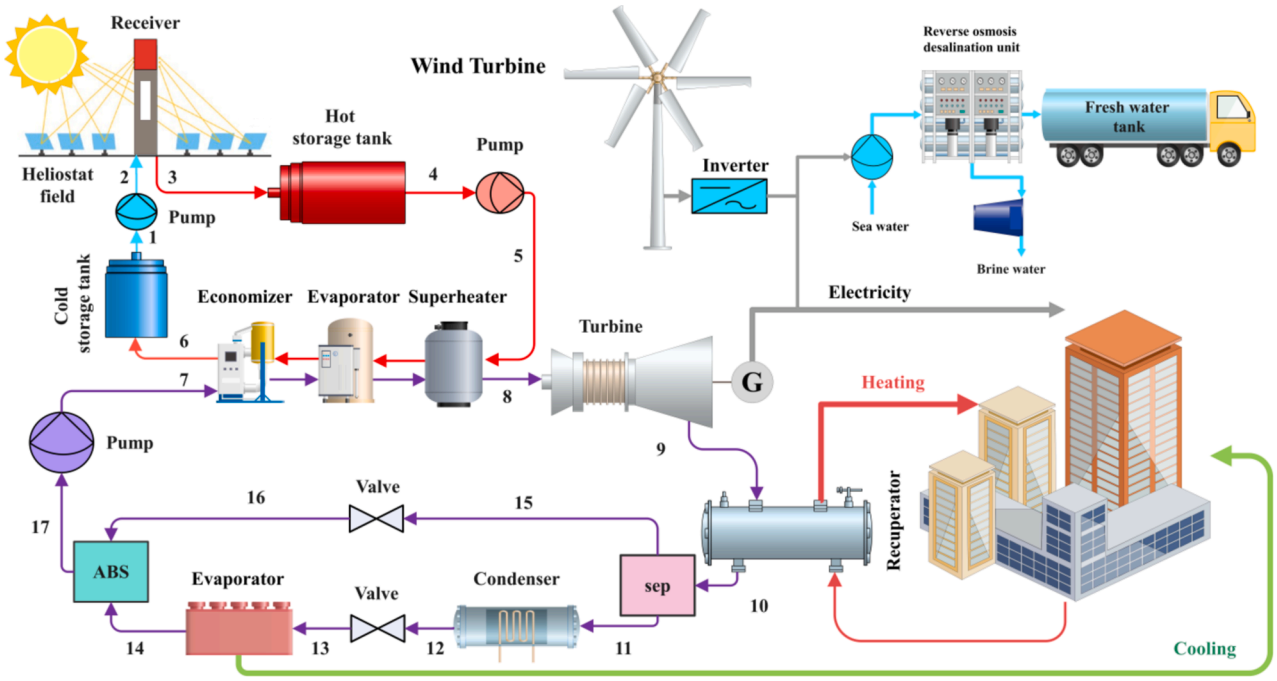

Fig. 15. Schematic of the Solar-Wind System.

Table 4
Principal Parameters of the NREL 5 MW Wind Turbine [40].

Values	Parameters
Power capacity	5 MW
Cut-in WS	3 m/s
Cut-out WS	25 m/s
Rated WS	11.4 m/s
Rotor radius (R)	63 *m*
Rated generator speed	122.9 rad/s
Rated generator torque	43093.55 N · m
Gearbox ratio	97:1
Maximum power coefficient	0.482

highlight its efficiency, energy production, and ecological footprint.

4.1. Validation

Validation is a fundamental step in scientific research, particularly when introducing a novel system. In this context, to verify and authenticate the work accomplished, specific attention was given to the RO desalination unit, an integral innovation within the solar-wind system. The validation process involved assessing the RO model by comparing it with the study conducted by Nafey and Sharaf [48]. Table 5 presents the key outcomes from this validation process, indicating a commendable level of accuracy in the modeling.

4.2. Multi-objective optimization (optimizing system performance)

4.2.1. Optimization methodology

RSM is utilized to optimize the cogeneration system whilst simultaneously cutting associated costs.

4.2.2. Optimization variables

Table 6 provides the key optimization parameters along with their defined ranges.

Optimization aims to enhance system performance and achieve the most efficient energy consumption for building within an optimal system state. This study utilized six decision variables and three objective functions to derive an optimal outcome, ultimately improving the system's technical efficiency. The study conducted 55 critical simulation runs, which were analyzed using Response Surface Methodology (RSM) with the aid of Design Expert software. This process optimized the cogeneration system's performance and identified optimal values for Objective Functions (OFs). Table 7 summarizes the optimal solution derived from RSM, a machine learning technique encompassing input parameters and objective functions. This analysis was based on a screening process within the employed Multi-Objective Optimization (MOO) method.

Fig. 20 depicts the influence of key design parameters on the production power objective function, represented using a color gradient where red indicates higher power production and green signifies lower outputs. Increasing the number of heliostats from 200 to 400 and turbine efficiency from 70 % to 90 % significantly enhances power generation, with the highest value reaching approximately 1,800 kWh, aligning closely with the predicted optimal output of 1,672.8 kWh. Similarly, a pump efficiency of 80 % combined with higher heliostat numbers around 400 yields near-optimal power outputs. For turbine efficiency, power increases from 1,200 kWh at an inlet pressure of 26.8053 kPa and efficiency below 80 %, to 1,400 kWh between 30 and 33.1947 kPa with efficiency near 80 %, and reaches 1,600 kWh at 36.3894 kPa and 86 % efficiency. For heliostat numbers, power rises from 800 kWh at 26.8053 kPa and 220 heliostats, to 1,000 kWh near 30 kPa and 245 heliostats, 1,200 kWh at 300 heliostats, 1,400 kWh at 350 heliostats, and peaks at 1,600 kWh at 33.1947 kPa and 370 heliostats. These findings confirm that heliostat number, turbine efficiency, and inlet pressure are critical variables for optimizing power generation in the cogeneration system, validating their roles in achieving the target performance metrics.

Fig. 21 displays the combined effect of two key input parameters on the heating production, represented with a red color gradient where red indicates higher production levels and green indicates lower levels. Optimization aims to maximize heating production, with a predicted optimal output of 8,760.03 kWh. The results demonstrate that increasing the number of heliostats from 200 to 400 significantly enhances the heating rate, particularly when turbine efficiency is close to 80 %. Heating output increases progressively from 5,000 kWh at 215 heliostats and 70 % efficiency to 9,000 kWh at 365 heliostats. Similarly,

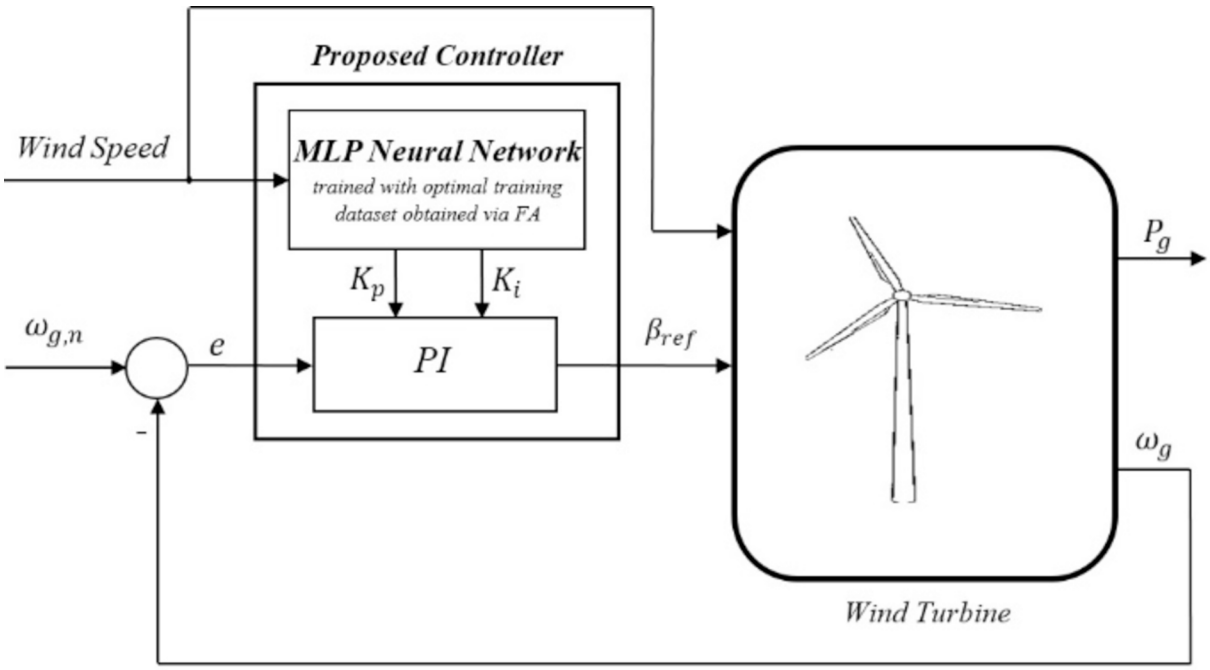

Fig. 16. Structure of the Suggested Pitch Controller.

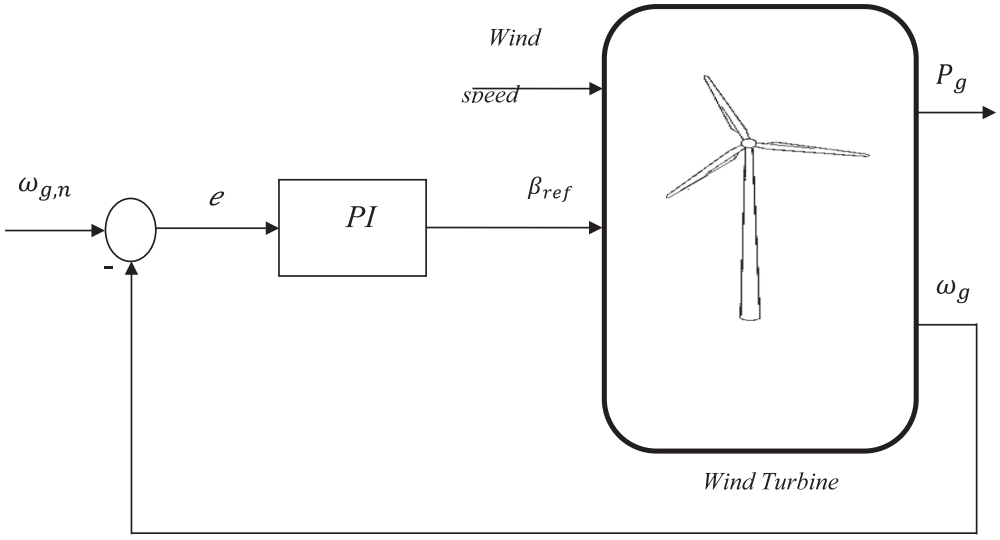

Fig. 17. Typical PI Pitches Controller Structure.

steam turbine inlet pressure (20–40 kPa) shows a notable effect, with 10,000 kWh achieved at 30 kPa when heliostat numbers reach 365. For the hot storage source temperature (723–823 K), the optimal range near 773 K corresponds to power outputs rising from 5,000 kWh at 215 heliostats to 9,000 kWh at 365 heliostats. Finally, pump efficiency at 80 % also correlates positively with increased heliostat numbers, contributing to similar trends in heating output. Among these parameters, the heliostat number has the most substantial impact, directly increasing the heating rate produced by the recuperator. These findings highlight the collective importance of the input variables in driving the system's heating production toward the optimization target, validating the effectiveness of the proposed cogeneration system.

In Fig. 22 illustrates the combined effect of critical inputs on the cooling production with red indicating higher production cooling levels and green representing lower levels. The optimization target is to achieve a predicted cooling output of 1,279.38 kWh. Among the design parameters, the number of heliostats, ranging from 200 to 400, has the most significant impact on cooling output. At an inlet pressure of 30 kPa, cooling production increases from 800 kWh at 245 heliostats to 1,200 kWh at 335 heliostats. Similarly, hot storage source temperature (723–823 K) influences cooling output, with optimal performance near 773 K and heliostat numbers increasing from 245 to 400, resulting in cooling outputs from 800 to 1,400 kWh. Turbine efficiency (70–90 %) further impacts cooling production, with outputs rising from 800 kWh at 245 heliostats to 1,200 kWh at 345 heliostats, peaking at 80 % efficiency. The relationship between hot storage source temperature and pump efficiency also shows cooling outputs decreasing from 1,300 kWh at 723 K to 1,150 kWh at 817 K at 80 % efficiency, reflecting the trade-off between efficiency and thermal input conditions. These findings highlight that the heliostat number exerts the strongest positive effect on cooling production through the evaporator, while all decision variables collectively contribute to achieving the system's cooling production

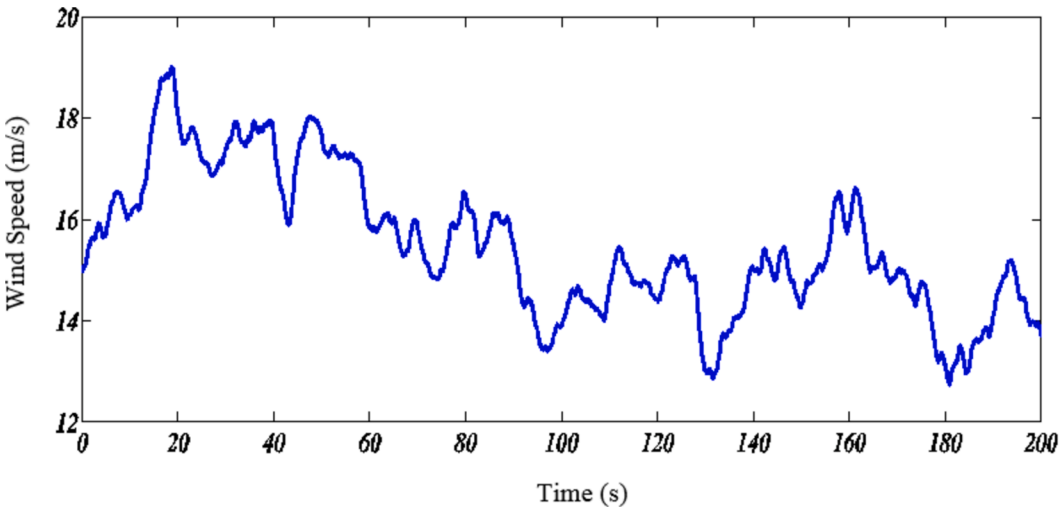

Fig. 18. Profile of Wind Speed based on 15 m/s Average.

target. The results validate the optimization strategy and emphasize the importance of balancing key parameters to enhance system performance.

4.3. Case study

Ahvaz, the largest city in Khuzestan province, experiences a hot climate with abundant sunshine, mild winters, and scorching summers, all of which significantly impact solar power system performance. This study analyzes power generation, cooling load, CO_2 emissions, and heating load, focusing on the influence of key weather parameters: T_o, WS, and SRI. Fig. 23 illustrates the system's energy production patterns across varying weather conditions. Fig. 23 (a) depicts the hourly variations in heating output, with the highest heat production from the recuperator occurring from late March to early September, as rising air temperatures drive increased thermal energy utilization. Fig. 23 (b) displays the hourly changes in cooling production, indicating peak cooling output during the same period, aligning with the hottest months of the year when cooling demands are at their highest. These trends demonstrate the system's ability to dynamically adjust to seasonal energy demands, ensuring efficient heating and cooling production during periods of extreme weather.

Fig. 24 illustrates the hourly fluctuations in the steam turbine's net electricity production in response to varying weather parameters. The solar system generates the thermal energy required to drive the steam turbine. The power generation rate significantly increases spanning from mid-March to mid-October. During this period, heightened solar radiation intensifies thermal energy absorption, enabling the solar system to transfer more energy to the MSRC for electricity production. This seasonal trend underscores the strong correlation between solar radiation levels and steam turbine output, highlighting the system's ability to capitalize on abundant solar energy during the warmer months to optimize power generation.

Fig. 25 illustrates the hourly variations in power produced by wind turbines under varying weather parameters, comparing wind turbine power with and without pitch angle control. The data shows that employing pitch angle control consistently increases power output by 4.08 % over 24 h, especially at higher wind speeds, by optimizing the blade's angle of attack to maintain the turbine's aerodynamic efficiency. The turbine efficiency improves from 56.90 % to 59.22 %, highlighting how pitch angle control enhances performance by optimizing the blade's interaction with wind flow. While this mechanism enhances power output, the standard deviation of power remains comparable, indicating that additional strategies, such as hybrid renewable setups, may be needed to further stabilize fluctuations and ensure grid reliability. Nonetheless, pitch angle control ensures the turbine operates closer to its rated capacity, maximizing energy production.

Fig. 26 displays the hourly fluctuations in the whole system's generated power across AT, WS, and SRI. The power output from the steam and wind turbines is balanced against the RO's energy usage and pumps, with the steam turbine utilizing solar energy and the wind turbine harnessing local wind resources. Employing pitch angle control in the wind turbine results in consistently higher overall system power outputs, with hourly improvements ranging from 1 kWh to 3 kWh compared to scenarios without control. This improvement particularly happens during moderate to high wind conditions, where it optimizes the aerodynamic efficiency of the blades. The cumulative system power over 24 h increases by 167,162 kWh, demonstrating its significant impact on energy production. This mechanism enhances stability during peak production periods by reducing losses and improves cumulative energy output over time. While the differences in output are minimal during low-production hours, the cumulative impact highlights the importance of pitch angle control in maximizing energy production and ensuring efficient system operation under fluctuating conditions.

In Fig. 27, the system's hourly freshwater production via the RO desalination unit is depicted against fluctuations in weather parameters. A unique aspect of this research involves leveraging the system's production power to generate freshwater, with the required power for the water softener sourced from the system's output, creating a direct link between electricity generation and freshwater production. The RO system's efficiency is evaluated under two conditions: with and without pitch angle control for the wind turbine. The data reveals that implementing pitch angle control results in a slight but consistent increase in hourly freshwater production, ranging from 0.01 to 0.05 (m^3/hour), depending on the weather conditions. Over 24 h, this results in a measurable increase in cumulative freshwater output, demonstrating the substantial impact of enhanced power generation on desalination efficiency. The stability of the RO system is also maintained across both scenarios, with pitch angle control ensuring more consistent production during high-output periods. These findings show the critical relationship between energy and water, illustrating how even small optimizations in power generation can significantly improve desalination performance.

Fig. 28 shows the hourly changes in energy efficiency concerning weather conditions. The efficiency is closely tied to the output power and the overall annual performance. Analysis indicates that implementing pitch control for the wind turbine improves the energy efficiency of the whole system by up to 0.032 % at specific hours, with an average improvement of 0.0011 % across the year. This indicates the role of pitch angle optimization in enhancing system performance under varying weather conditions.

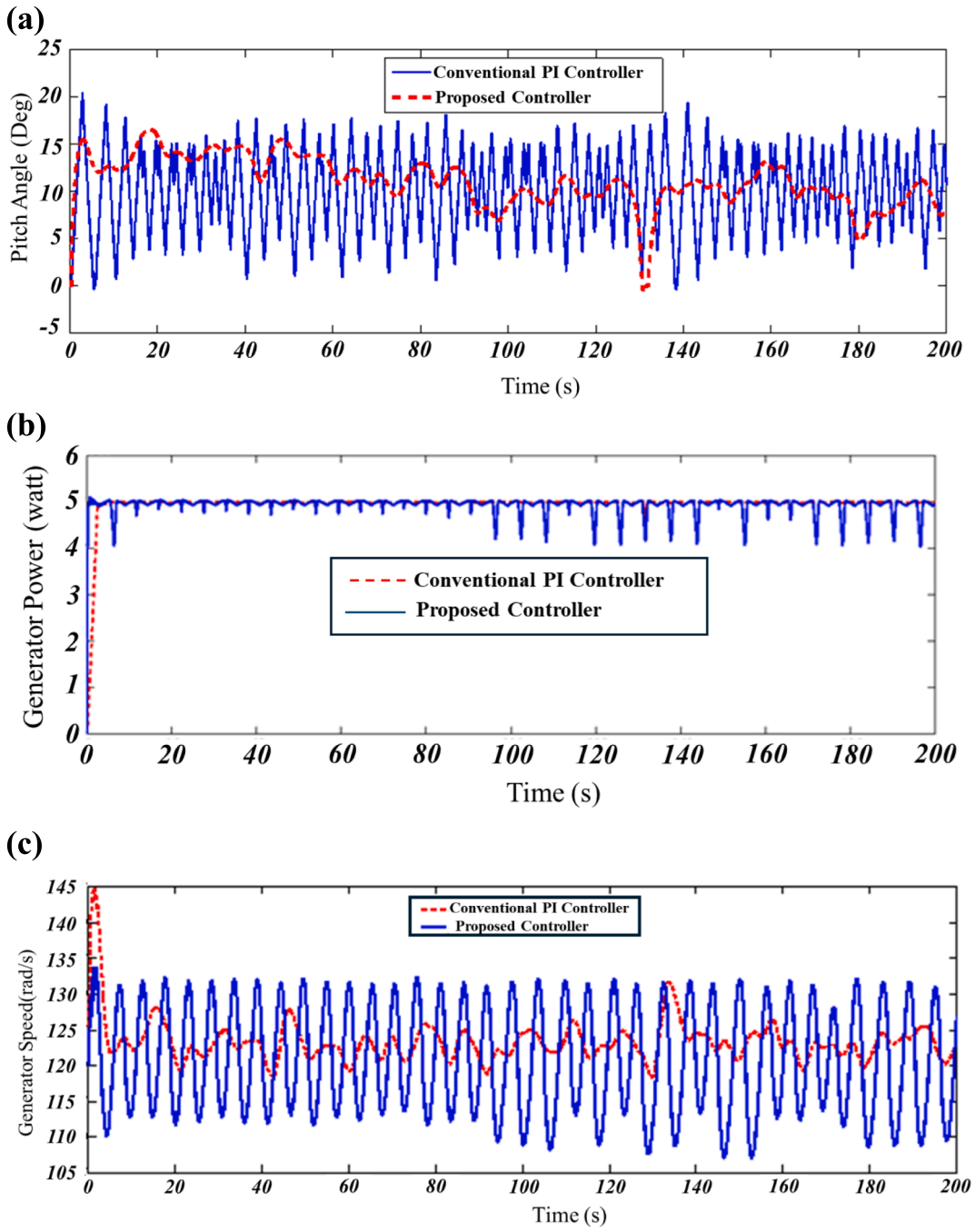

Fig.19. Proposed vs. Conventional PI Controller: (a) Pitch Angle Changes, (b) Generator Output Power Stability, and (c) Generator Speed Fluctuations.

Table 5
Validation Results [48].

Parameter	Current Study	Referenced Study	Differentiation (%)
$\dot{W}_{pump.RO}$	1120	1131 (kW)	0.97
M_f	485.9	485.9 (m^3/h)	0
SR	0.9944	0.9944	0
X_b	64,180	64,180 (ppm)	0
X_d	252	250 (ppm)	0.8
ΔP	6843	6850 (kPa)	0.1

Table 6
Optimization Parameters and Defined Ranges.

Name	Lower Limit	Upper Limit
Pump efficiency	0.7	0.9
Turbine efficiency	0.7	0.9
Heliostat number	200	400
Inlet pressure to steam turbine	20	40
Cold storage source temperature	523	623
Hot storage source temperature	723	823

Fig. 29 illustrates the changes in the energy efficiency rate or Exergy Round Trip Efficiency (ERTE) across changing weather parameters. The analysis reveals an association between exergy efficiency and power generation, with fluctuations influenced by AT, WS, and SRI. The data shows that the mean ERTE values were 58.90 % without pitch control and 47.15 % with pitch control, reflecting an average change of −11.75 %. The differences ranged from −10.77 % to −12.66 %, indicating that

Table 7
Optimal Values.

Pump efficiency (%)	0.82
Turbine efficiency (%)	0.86
Heliostat number (−)	363
Inlet pressure (kPa) steam turbine	36.38
Cold storage source temperature (^{0}C)	542.12
Hot storage source temperature (^{0}C)	741.05
Output net power (kWh)	1672.8
Heating (kWh)	8760.02
Cooling (kWh)	1279.38
Desirability	0.87

pitch control adjustments consistently reduced ERTE. These results highlight the role of pitch control in stabilizing energy output under varying weather conditions while prioritizing consistent system performance over peak efficiency. Such insights are crucial for optimizing renewable energy systems in dynamic environments.

Fig. 30 illustrates the ecological advantages of system design. Regular power plants emit about 0.204 tons of CO_2 per 1 MWh of electricity generated. The figure quantifies the hourly CO_2 emissions reduction achieved by generating clean electricity. With conventional power plants incurring $24 per ton of CO_2 in environmental costs, the solar-wind system installation offers significant cost savings by preventing such emissions. This approach not only reduces CO_2 emissions but also promotes the growth of green spaces, highlighting the cost benefits of using solar-wind power [40].

The system's implementation presents an opportunity to mitigate annual environmental costs, equivalent to the expansion of green spaces and vegetation. It's important to note an estimated valuation of $4,940/hectare, reflective of the average non-waterfront bottomland habitat [40,57]. Table 8 details the annual environmental performance of the Ahvaz system concerning power generation from two steam turbines and a wind turbine employing pitch angle control.

The findings demonstrate that implementing pitch angle control elevates the wind turbine's net generated power, subsequently positively impacting the overall system output derived from the combined power of both the wind and steam turbines. Moreover, implementing pitch angle control correlates with increased energy and exergy efficiencies, attributed to its direct influence on production power. It underscores the integration of pitch angle control in the calculations.

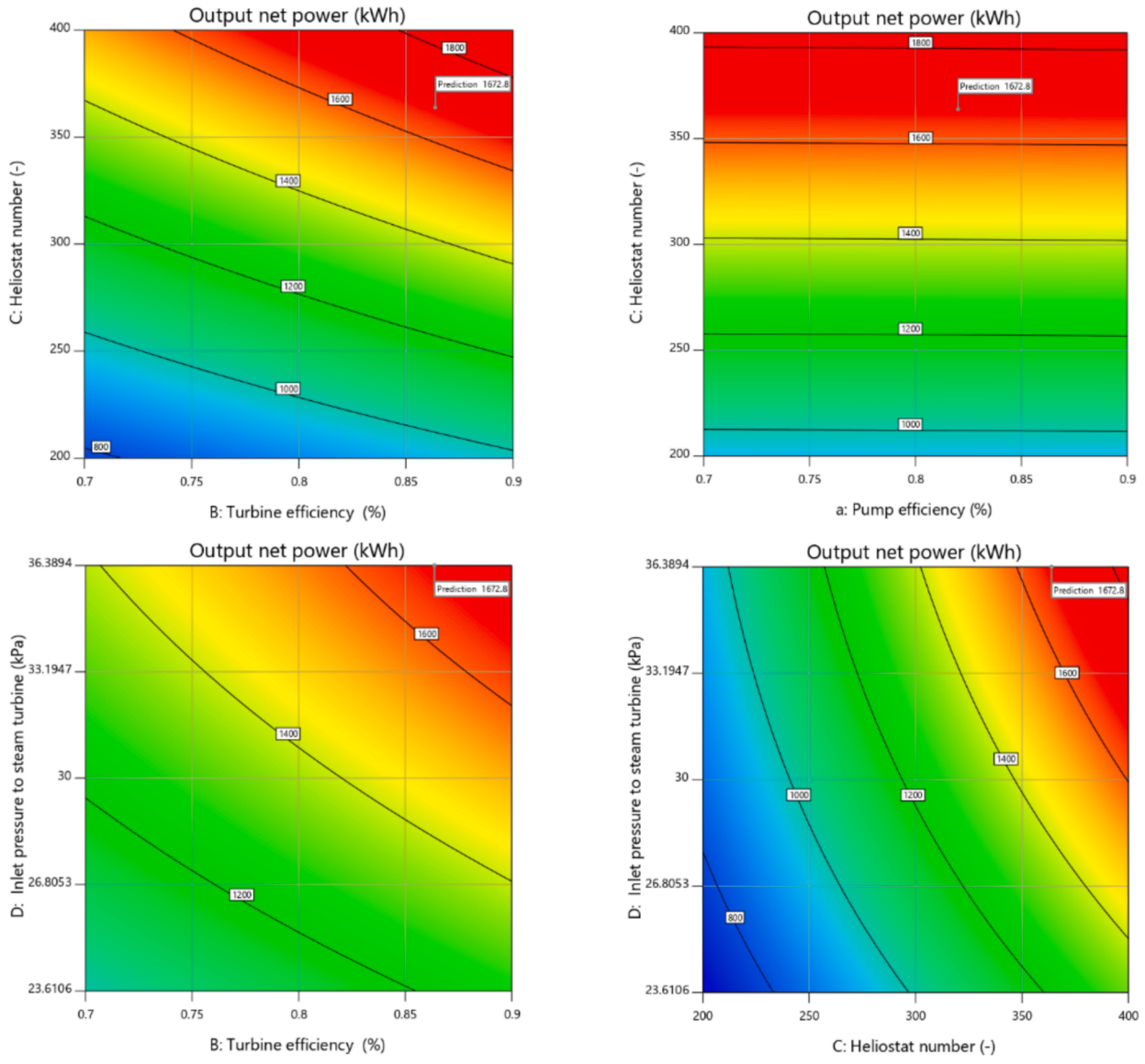

Fig. 20. Impacts of Inputs on Power Production.

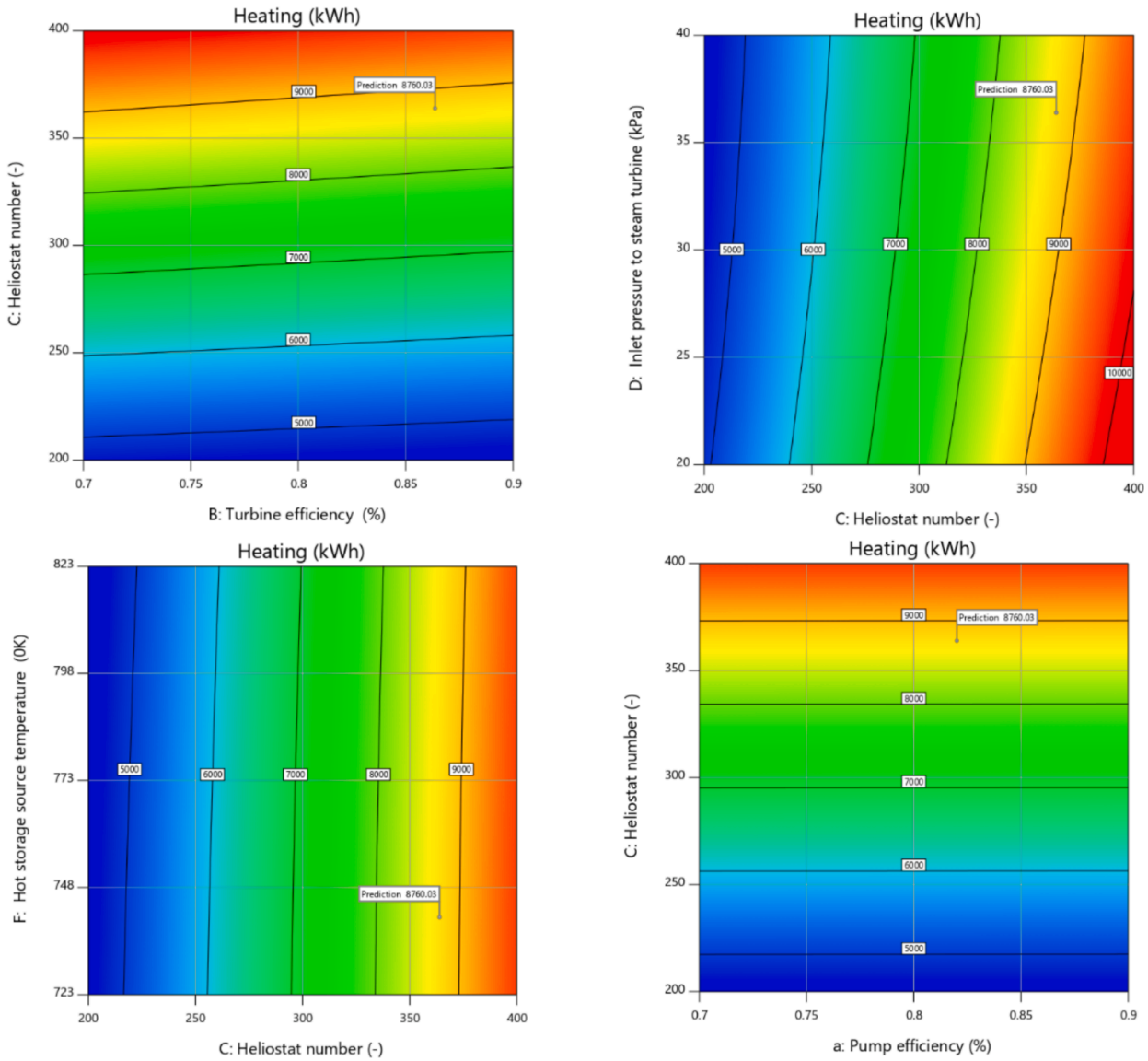

Fig. 21. Impacts of Inputs on Heating Production.

4.4. Proposed system capability

The performance of the proposed system in meeting the energy demands of the simulated residential building in Ahvaz is analyzed under annual weather variations. The comparison between electricity usage and generation by the system (Fig. 31a) over a year highlights its ability to consistently meet the building's power needs across different conditions. Similarly, the cooling demand of the simulated building is evaluated against the cooling energy generated by the cogeneration system (Fig. 31b), showing effective performance during peak summer months when cooling requirements are at their highest. The heating demand is finally compared with the system's heating energy production (Fig. 31c), demonstrating its capability to adapt to fluctuating heating requirements, particularly during the cooler months of the year. These analyses prove the system's reliability and adaptability in addressing the diverse energy needs of residential buildings in Ahvaz's climate.

4.5. Comparison with previous studies

The findings of this study were compared with previous works on renewable energy systems and NZEBs. Table 9 outlines the key metrics, including energy efficiency, exergy efficiency, CO2 reduction, and key findings or innovations, for each study.

Table 9 highlights the strengths of the current study's hybrid solar-wind co-generation system with an MSRC and RO desalination unit. Achieving energy and exergy efficiencies of 33.05 % and 34.02 %, respectively, and an annual CO_2 reduction of 1,334.47 tons, the system demonstrates acceptable performance metrics, particularly in its ability to produce electricity, heating, cooling, and freshwater for a large-scale residential application in severe hot climates. While the energy and exergy efficiencies are slightly lower than smaller systems optimized for specific outputs, such as hydrogen production or PV-only applications, the results are competitive considering the comprehensive functionality and larger size of the system. The innovative integration of pitch angle control, surplus energy storage, and co-generation capability optimizes resource utilization and supports the system's robust performance under extreme climatic conditions. This multi-functional approach, adopted to address diverse energy demands on a scale, confirms the system's viability and effectiveness in achieving net-zero energy goals while maintaining ecological and economic sustainability.

4.6. Stored energy

Fig. 32 illustrates the hybrid solar-wind system's ability to effectively

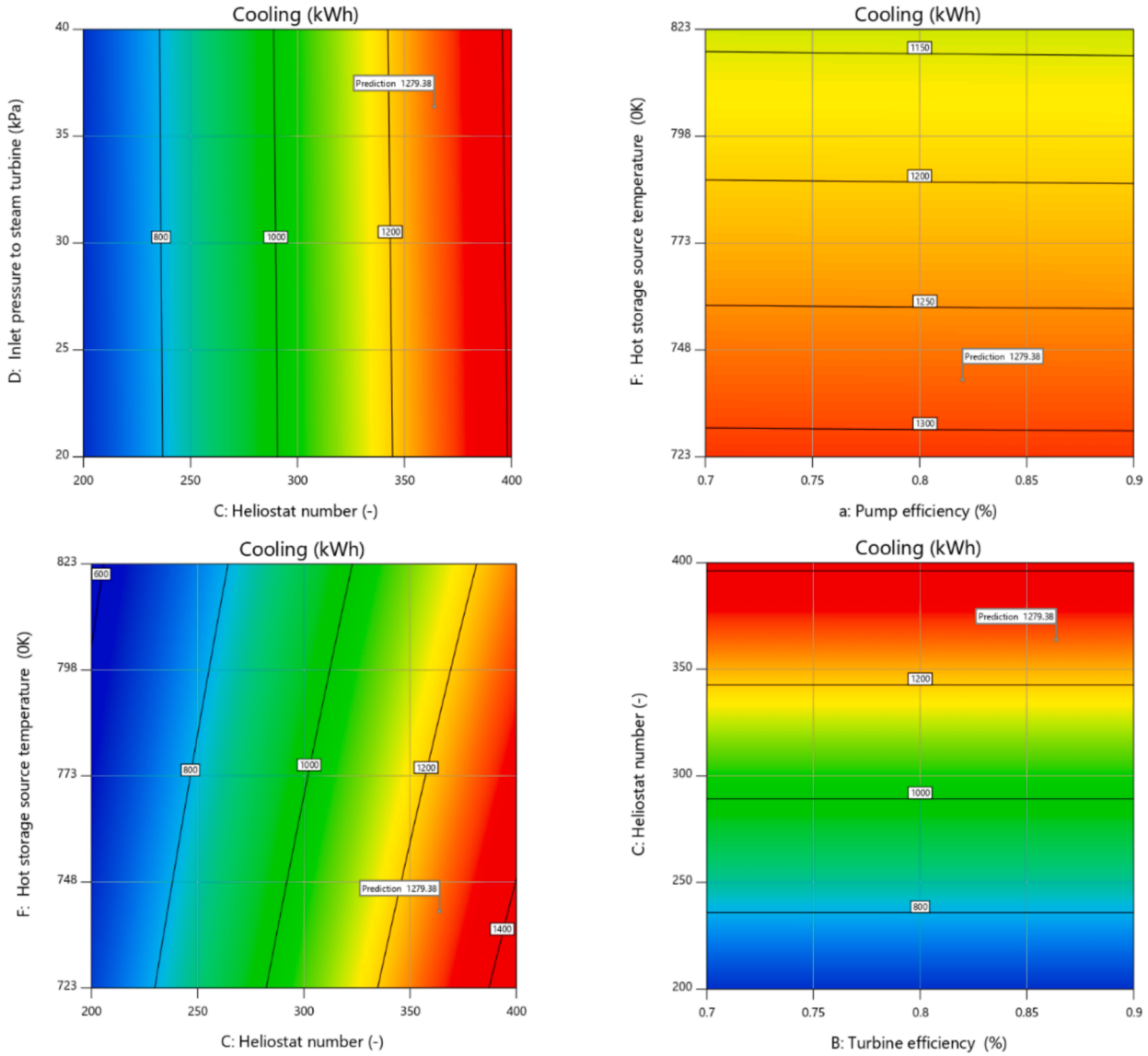

Fig. 22. The Effect of Two Inputs on the Cooling Production.

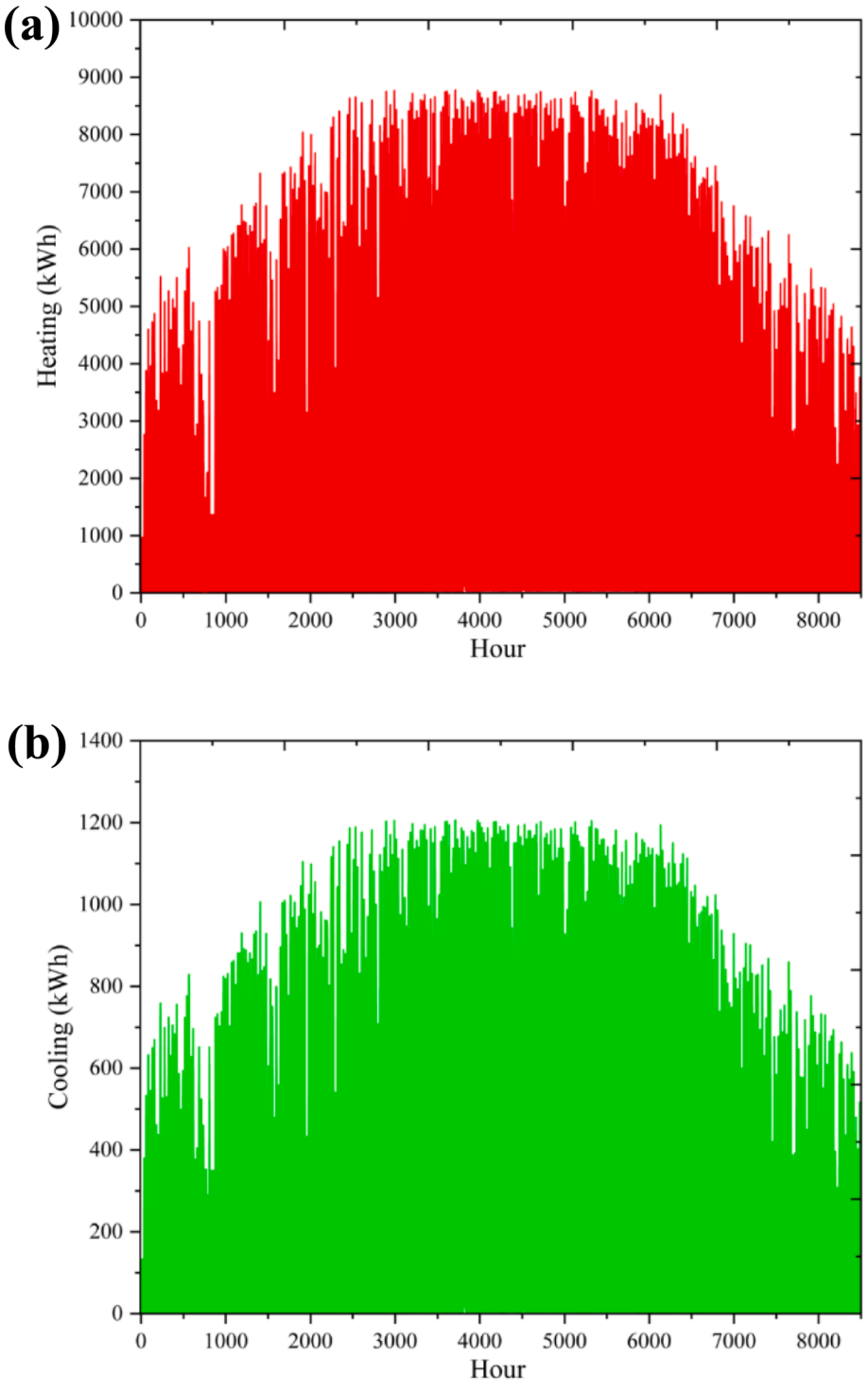

Fig. 23. Hourly (a) Heating and (b) Cooling production Adjustments Influenced by Weather Conditions.

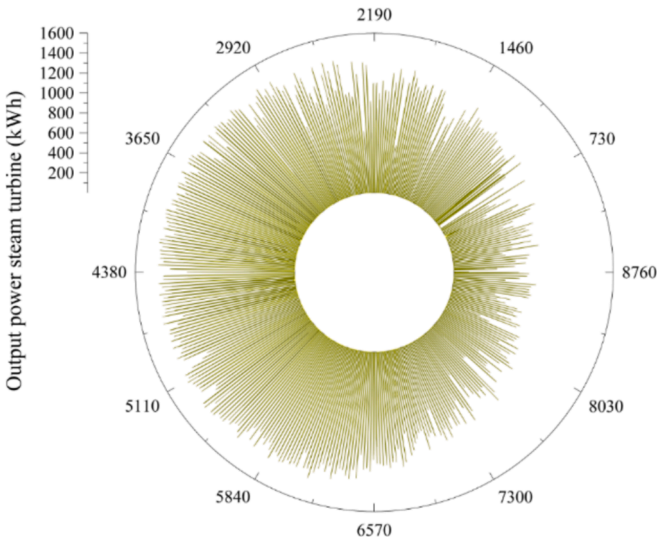

Fig. 24. Hourly Fluctuations in Steam Turbine Power Output in Response to Weather Changes.

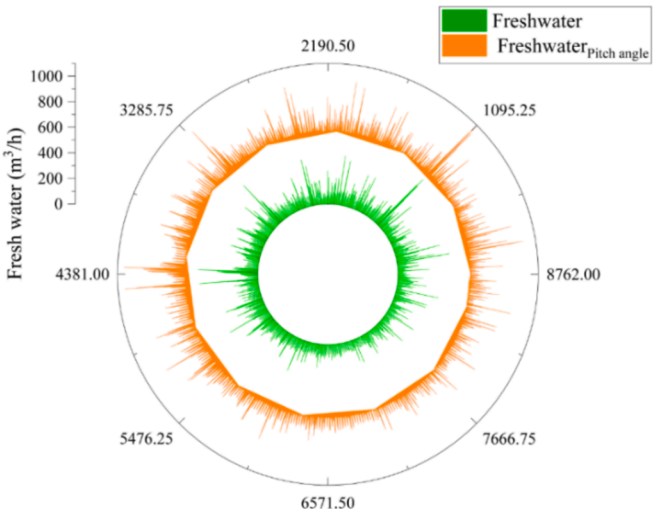

Fig. 27. Hourly Freshwater Production via RO with and Without Pitch Angle Control.

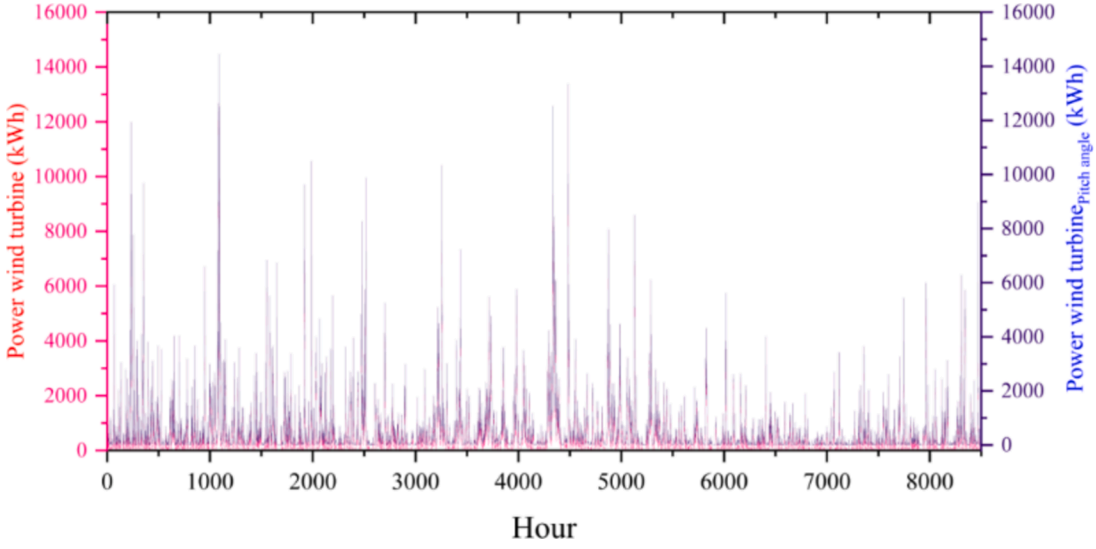

Fig. 25. Hourly Variations in Wind Turbine Power Output with and without Pitch Angle.

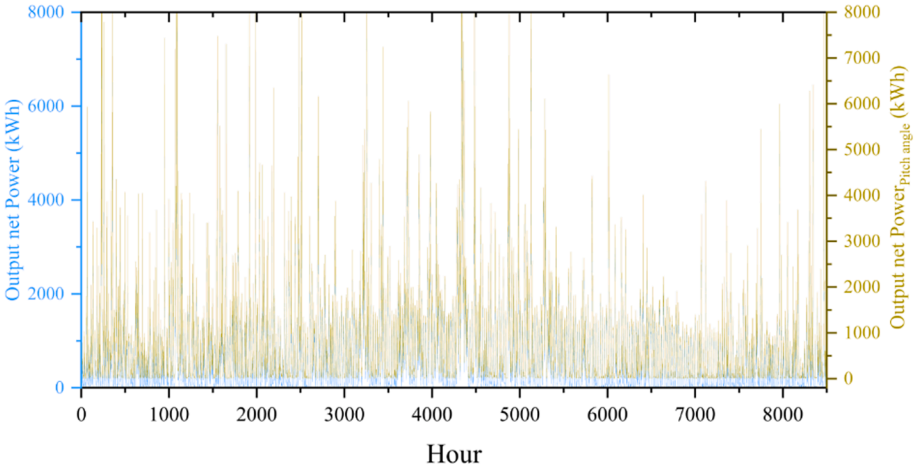

Fig. 26. Hourly Fluctuations in System Production Power with and Without Pitch Angle Control.

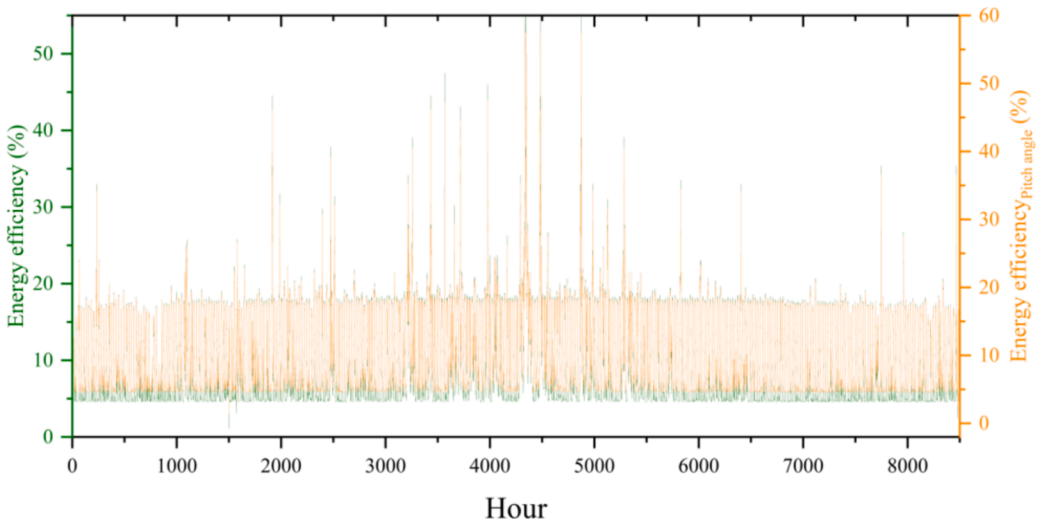

Fig. 28. Hourly Energy Efficiency Variations by Pitch Angle and Weather Conditions.

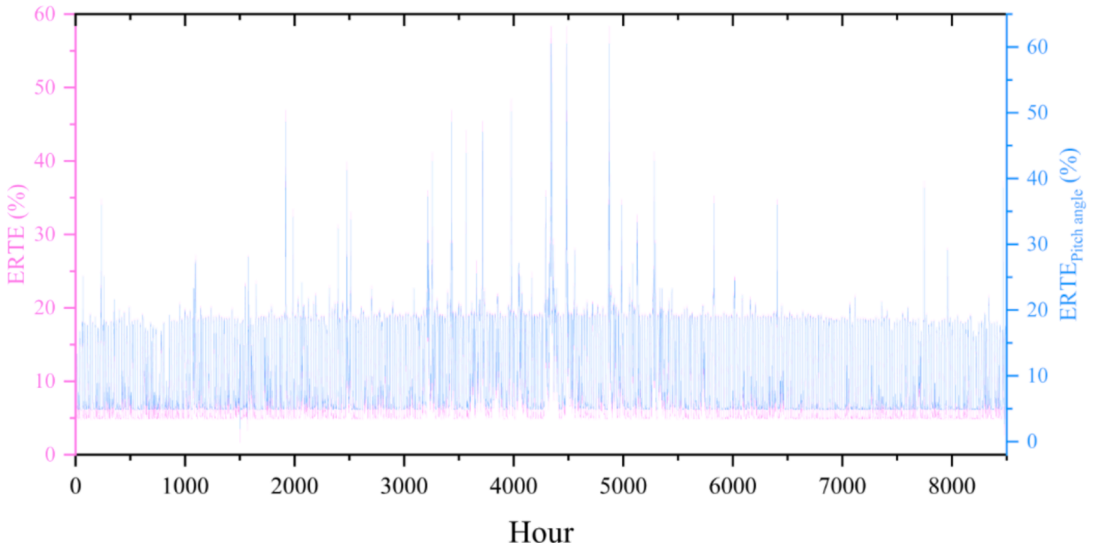

Fig. 29. Hourly changes in the ERTE Relative to Pitch Angle and Weather Parameters.

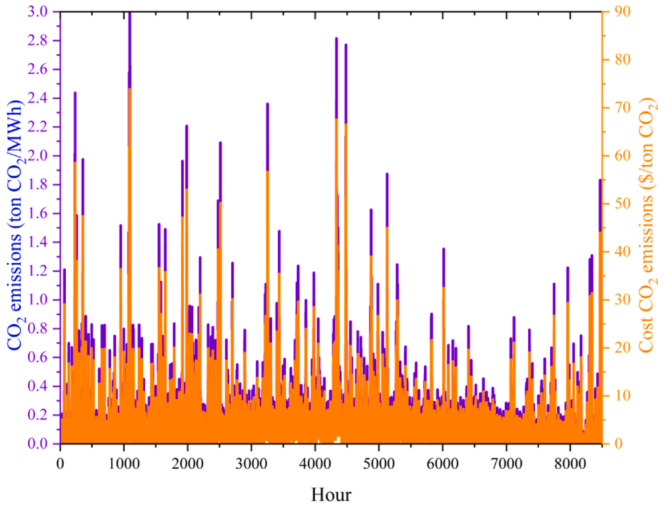

Fig. 30. CO_2 Emission Reduction and Cost Savings from the Solar-Wind System.

Table 8
Annual Environmental Performance of the Ahvaz System.

Output Power	The amount of CO_2	The Cost of CO_2	Hectares
6541.56	1334.47	32027.47	6

fulfill the energy demands of residential buildings. Beyond meeting primary energy needs, the system generates excess electricity, cooling, and heating that can be stored for diverse uses or sold back to the national grid. The hourly tracking shows that stored heating ranges from 8,345 to 8,374 kWh, with an average of 8,359 kWh, contributing to a total of 73,224,805 kWh annually. Similarly, stored cooling varies between 1,147 and 1,151 kWh, averaging 1,149 kWh, and accumulating a total of 10,062,451 kWh annually. These insights demonstrate the system's capacity for efficient energy storage, supporting both immediate and long-term energy needs.

5. Limitations and future direction

The current study demonstrates the feasibility of a hybrid solar-wind

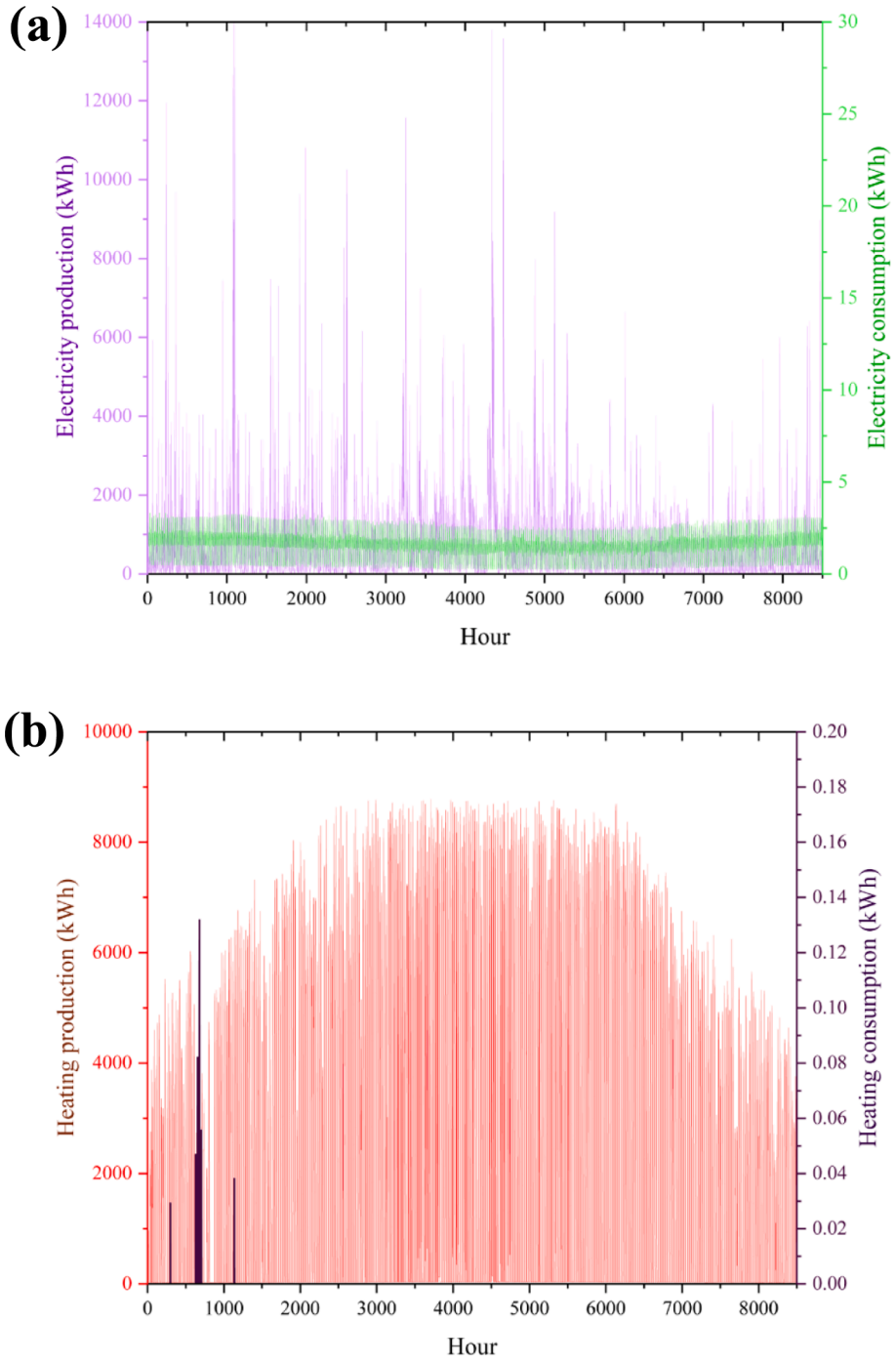

Fig. 31. Comparison of Energy Production vs Consumption (a) Electricity, (b) Heating, and (c) Cooling.

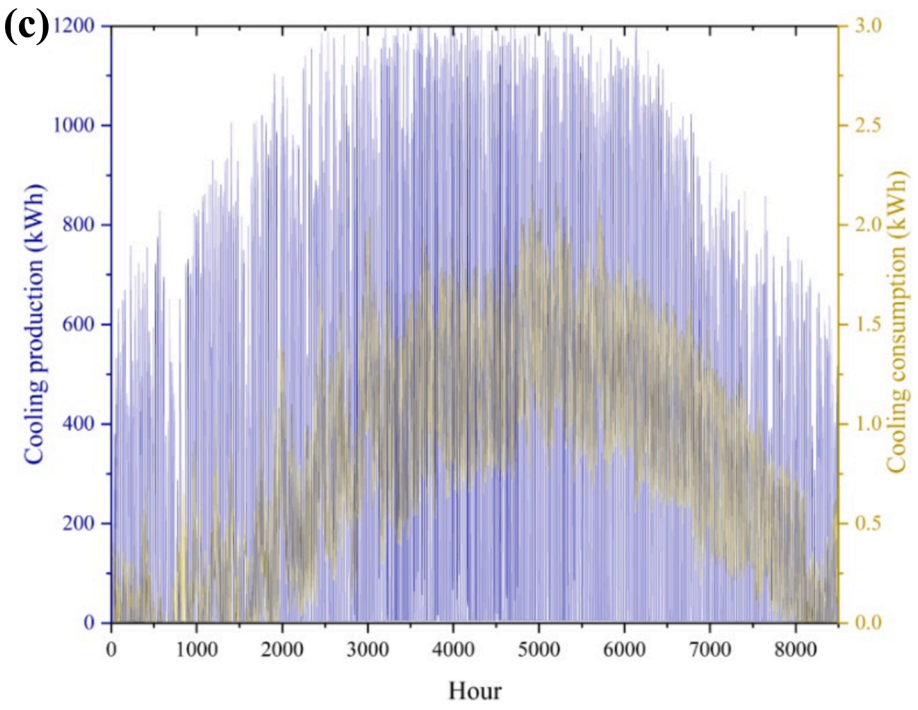

Fig. 31. (*continued*).

Table 9
Annual Environmental Performance of the Ahvaz System.

Authors [Reference]	System Description	Energy Efficiency (%)	Exergy Efficiency (%)	CO_2 Reduction (tons/year)	Key Findings and Notes
Current Study	Hybrid solar-wind co-generation with MSRC and RO	33.05	34.02	1,334.47	Achieves higher efficiencies with innovative pitch angle control; substantial freshwater and energy surplus.
Nikitin, Andrey, et al. [58]	Solar-wind multi-generation with TES and HESS	33.51	27.07	20.34 (max)	Demonstrates lower CO_2 reduction and exergy efficiency; economic analysis included.
Yilmaz, Fatih. [28]	Hydropower, wind, PEM, RO	61.29	57.14	Not reported	Shows remarkably higher efficiencies but focuses on different outputs, e.g., hydrogen production
Rong, Fanhua, et al. [59]	Solar-wind-hydrogen for CCHP and desalination	48.49	19.98	Not reported	High energy efficiency; parametric optimization of solar/wind and hydrogen systems.
Arslan, Erhan, et al. [60]	PV panels under extreme climate	11.35 (max)	10.25 (max)	3.06 kg/day (1.12 tons/year)	Focused on optimizing PV modules using meteorological parameters and statistical methods.

co-generation system in addressing the energy demands of residential buildings situated in a severe hot climate. However, certain limitations must be acknowledged. First, the analysis primarily focuses on ideal operating conditions and assumes constant efficiencies for key system components, which may not fully reflect the variations encountered in real-world applications. Second, the study does not account for long-term degradation of the system components, such as photovoltaic panels and wind turbines, or their associated maintenance needs, which could impact the system's overall performance. Finally, while the study evaluates energy performance on an annual scale, the lack of a detailed cost-benefit analysis limits insights into the economic feasibility of scaling the system for broader applications.

Future research could address these limitations by incorporating simulations that capture the dynamic performance of the proposed system under real-world conditions and varying operational scenarios. Integrating adaptive control mechanisms, such as Artificial Intelligence (AI)-based optimization, could enhance the system's ability to respond to fluctuating environmental factors and varying load demands. Future work could also refine the analysis by incorporating dynamic solar efficiency models that account for environmental variations and panel degradation. This enhancement would provide a more detailed understanding of solar system performance and support practical implementation in diverse climates. Moreover, extending the study to assess long-term durability and economic implications, including lifecycle costs and return on investment, would provide a more comprehensive evaluation of the system's scalability. Examining the hybrid system within smart urban grids could enable district-level applications, further contributing to sustainable energy solutions for urban communities. Future work can also consider simulations across diverse climates, such as temperate or cold regions, to validate the adaptability of the system. Developing generalized performance models based on climatic parameters would enhance the applicability of the findings in a global context.

6. Conclusion

This study presents a co-generation system designed for a 3-unit Zero-Energy Building located in the hot climate of Ahvaz, Iran, integrating a Modified Steam Rankine Cycle, wind turbines, and solar units to produce electricity, heating, cooling, and freshwater. By using BEopt for energy modeling and the Engineering Equation Solver for energy and exergy analyses, the system ensures clean power production and meets diverse residential demands: 12,145 kWh for electricity, 0.94 kWh for heating, and 6,023 kWh for cooling, through carefully optimized load supply mechanisms, including a RO desalination unit. The implementation of optimization techniques, such as pitch angle control, significantly enhances wind turbine performance, resulting in reduced

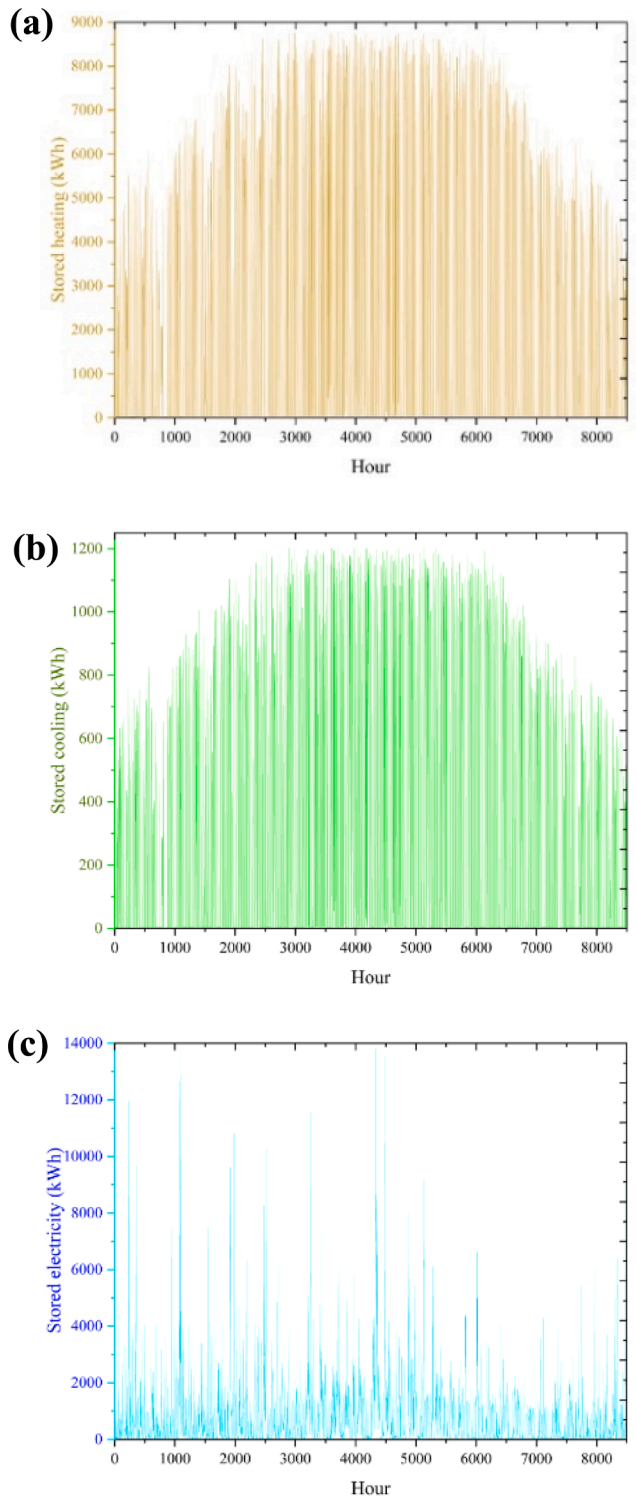

Fig. 32. Hourly Tracking of Stored (a) Heating, (b) Cooling, and (c) Electricity.

carbon emissions by 1,334.47 tons per year, improved ecological sustainability, and achieved energy and exergy efficiencies of 33.05 % and 34.02 %, respectively. The system's peak capacities were 1,672 kWh (electricity), 8,760 kWh (heating), and 1,279 kWh (cooling), while annual outputs exceeded residential demands with 6,541,564 kWh of electricity, 14,717,841 kWh of heating, 2,023,099 kWh of cooling, and 380,858 m3 of freshwater. These surpluses enable the selling of 6,529,419 kWh of electricity to the grid and offset costs with 14,717,840 kWh of heating and 2,017,076 kWh of cooling. The research demonstrates that integrating solar and wind technologies within advanced optimization frameworks, such as Response Surface Methodology, can fulfill Zero-Energy Building targets, mitigate environmental impacts, and maintain scalability in severe climates and diverse building types. Future work could address dynamic optimization, the application of surplus thermal energy for agriculture or water recycling, and the long-term durability and scalability of system components.

The key findings of this research are:

- The co-generation system meets and exceeds Zero-Energy Building energy demand in severe climates, balancing energy supply, storage, and surplus for sustainability.
- Integrating solar and wind energy with advanced optimization techniques, such as Response Surface Methodology, achieves high energy (33.05 %) and exergy (34.02 %) efficiencies, optimizing multi-functional renewable energy systems.
- Using pitch angle control enhances wind turbine performance, ensuring consistent outputs under varying climatic conditions and reducing CO_2 emissions by 1,334.47 tons annually.
- The system provides electricity, heating, cooling, and freshwater, demonstrating the versatility of hybrid renewable energy systems for residential and community needs.
- Generating surplus energy for grid export (6,529,419 kWh) and utilizing excess thermal energy reduces operational costs, supporting economic scalability in diverse settings.
- Integrating renewable energy with desalination addresses water scarcity, energy sustainability, and environmental challenges, offering a foundation for ZEB innovation.

Declaration of competing interest

During the preparation of this work, the authors used an OpenAI tool to enhance language and readability. After using the tool, the authors reviewed and edited the content as needed. They take full responsibility for the final content of the publication. The authors highlight that AI's role was to assist in refining the text and language, and not to replace any critical tasks of the authors.

Acknowledgment

This work was supported by the National Research Foundation of Korea (NRF) grant funded by the Korea government (MSIT) (2021R1A2C1092152).

Data availability

Data will be made available on request.

References

[1] R.K. Jaysawal, et al., *Concept of net zero energy buildings (NZEB)-A literature review*, Cleaner Eng. Technol. 11 (2022) 100582.
[2] I. Razzaq, et al., *Reduction in energy consumption and CO2 emissions by retrofitting an existing building to a net zero energy building for the implementation of SDGs 7 and 13*, Front. Environ. Sci. 10 (2023) 1028793.
[3] A. Ahmed, et al., *Assessment of the renewable energy generation towards net-zero energy buildings: A review*, Energ. Buildings 256 (2022) 111755.
[4] F.M. Butera, *Zero-energy buildings: the challenges*, Adv. Build. Energy Res. 7 (1) (2013) 51–65.
[5] J. Wei, et al., *Hot topics and trends in zero-energy building research—A bibliometrical analysis based on CiteSpace*, Buildings 13 (2) (2023) 479.
[6] J. Lizana, et al., *Advances in thermal energy storage materials and their applications towards zero energy buildings: A critical review*, Appl. Energy 203 (2017) 219–239.
[7] M. Hawks, S. Cho, *Review and analysis of current solutions and trends for zero energy building (ZEB) thermal systems*, Renew. Sustain. Energy Rev. 189 (2024) 114028.
[8] H.-L. Lou, S.-H. Hsieh, *Towards Zero: A Review on Strategies in Achieving Net-Zero-Energy and Net-Zero-Carbon Buildings*, Sustainability 16 (11) (2024) 4735.
[9] K.-Y. Lo, J.H. Yeoh, I.-Y.-L. Hsieh, *Towards nearly zero-energy buildings: Smart energy management of vehicle-to-building (V2B) strategy and renewable energy sources*, Sustain. Cities Soc. 99 (2023) 104941.

[10] V.J. Reddy, et al., *Pathway to sustainability: An overview of renewable energy integration in building systems*, Sustainability 16 (2) (2024) 638.
[11] W. Lyu, et al., *Energy-efficient fresh air system with pressure-independent dampers for nearly zero energy buildings*, Appl. Therm. Eng. 234 (2023) 121240.
[12] T. Wilberforce, et al., *A review on zero energy buildings–Pros and cons*, Energy Built Environ. 4 (1) (2023) 25–38.
[13] Mohammed, B.U., et al., *Pathways for efficient transition into net zero energy buildings (nZEB) in Sub-Sahara Africa. Case study: Cameroon, Senegal, and Côte d'Ivoire.* Energy and Buildings, 2023. **296**: p. 113422.
[14] M. Shirinbakhsh, L.D. Harvey, *Feasibility of achieving net-zero energy performance in high-rise buildings using solar energy*, Energy Built Environ. 5 (6) (2024) 946–956.
[15] S. Mousavi, et al., *Data-driven prediction and optimization toward net-zero and positive-energy buildings: A systematic review*, Build. Environ. 242 (2023) 110578.
[16] A. Ye, et al., *Using solar energy to achieve near-zero energy buildings in Tibetan Plateau*, Renew. Energy 218 (2023) 119347.
[17] A.Q. Al-Shetwi, *Sustainable development of renewable energy integrated power sector: Trends, environmental impacts, and recent challenges*, Sci. Total Environ. 822 (2022) 153645.
[18] M. Ahmadizadeh, et al., *Technological advancements in sustainable and renewable solar energy systems*, in: *Highly Efficient Thermal Renewable Energy Systems*, CRC Press, 2024, pp. 23–39.
[19] A.D.A. Bin Abu Sofian, et al., *Machine learning and the renewable energy revolution: Exploring solar and wind energy solutions for a sustainable future including innovations in energy storage*, Sustain. Dev. (2024).
[20] M. Gür, H.F. Öztop, F. Selimefendigil, *Analysis of solar underfloor heating system assisted with nano enhanced phase change material for nearly zero energy buildings approach*, Renew. Energy 218 (2023) 119265.
[21] T. Salameh, et al., *Analysis of cooling load on commercial building in UAE climate using building integrated photovoltaic façade system*, Sol. Energy 199 (2020) 617–629.
[22] Y. Varol, H.F. Oztop, *Buoyancy induced heat transfer and fluid flow inside a tilted wavy solar collector*, Build. Environ. 42 (5) (2007) 2062–2071.
[23] Q. Hassan, et al., *A review of hybrid renewable energy systems: Solar and wind-powered solutions: Challenges, opportunities, and policy implications.* Results, Engineering (2023) 101621.
[24] A. Sayigh, *Solar and wind energy will supply more than 50% of world electricity by 2030. Transition towards a Carbon Free Future: Selected Papers from the World Renewable Energy Congress (WREC) 2023*, Springer, 2024.
[25] W. Zhang, et al., *A critical review of the performance evaluation and optimization of grid interactions between zero-energy buildings and power grids*, Sustain. Cities Soc. 86 (2022) 104123.
[26] P. Das, V. Chandramohan, *A review on recent advances in hybrid solar updraft tower plants: Challenges and future aspects*, Sustainable Energy Technol. Assess. 55 (2023) 102978.
[27] E. Assareh, et al., *Performance analysis of solar-assisted-geothermal combined cooling, heating, and power (CCHP) systems incorporated with a hydrogen generation subsystem*, Journal of Building Engineering 65 (2023) 105727.
[28] F. Yilmaz, *Design and performance analysis of hydro and wind-based power and hydrogen generation system for sustainable development*, Sustainable Energy Technol. Assess. 64 (2024) 103742.
[29] A. Emrani, A. Berrada, *A comprehensive review on techno-economic assessment of hybrid energy storage systems integrated with renewable energy*, J. Storage Mater. 84 (2024) 111010.
[30] N. Campion, et al., *Techno-economic assessment of green ammonia production with different wind and solar potentials*, Renew. Sustain. Energy Rev. 173 (2023) 113057.
[31] E. Assareh, et al., *Techno-economic analysis of combined cooling, heating, and power (CCHP) system integrated with multiple renewable energy sources and energy storage units*, Energ. Buildings 278 (2023) 112618.
[32] E. Assareh, A. Ershadi, M. Lee, *An integrated system for producing electricity and fresh water from a new gas-fired power plant and a concentrated solar power plant–Case study–(Australia, Spain, South Korea, Iran)*, Renewable Energy Focus 44 (2023) 19–39.
[33] G.-C. Ding, J. Peng, G. Mei-Yun, *Technical assessment of Multi-generation energy system driven by integrated renewable energy Sources: Energetic, exergetic and optimization approaches*, Fuel 331 (2023) 125689.
[34] Y. Cao, et al., *Development and transient performance analysis of a decentralized grid-connected smart energy system based on hybrid solar-geothermal resources, Techno-Economic Evaluation.* Sustainable Cities and Society 76 (2022) 103425.
[35] Acar, C., E. Erturk, and I. Firtina-Ertis, *Performance analysis of a stand-alone integrated solar hydrogen energy system for zero energy buildings.* international journal of hydrogen energy, 2023. **48**(5): p. 1664-1684.
[36] F. Musharavati, et al., *Multi-objective optimization of a biomass gasification to generate electricity and desalinated water using Grey Wolf Optimizer and artificial neural network*, Chemosphere 287 (2022) 131980.
[37] Y. Chen, et al., *Energy, exergy, and economic analysis of a centralized solar and biogas hybrid heating system for rural areas*, Energ. Conver. Manage. 276 (2023) 116591.
[38] H. Shakibi, et al., *Exergoeconomic and optimization study of a solar and wind-driven plant employing machine learning approaches; a case study of Las Vegas city*, J. Clean. Prod. 385 (2023) 135529.
[39] H. Braas, et al., *District heating load profiles for domestic hot water preparation with realistic simultaneity using DHWcalc and TRNSYS*, Energy 201 (2020) 117552.
[40] S.M. Alirahmi, et al., *A comprehensive techno-economic analysis and multi-criteria optimization of a compressed air energy storage (CAES) hybridized with solar and desalination units*, Energ. Conver. Manage. 236 (2021) 114053.
[41] M. Lu, et al., *Operational optimization of district heating system based on an integrated model in TRNSYS*, Energ. Buildings 230 (2021) 110538.
[42] M. Jafarian, et al., *Energy, economic, and environmental analysis of combined cooling, heat, power and water (CCHPW) system incorporated with photovoltaic/thermal collectors and reverse osmosis systems*, Journal of Building Engineering 75 (2023) 107059.
[43] A. Dezhdar, et al., *Transient optimization of a new solar-wind multi-generation system for hydrogen production, desalination, clean electricity, heating, cooling, and energy storage using TRNSYS*, Renew. Energy 208 (2023) 512–537.
[44] S. Sayadi, et al., *Analyzing the climate-driven energy demand and carbon emission for a prototype residential nZEB in central Sweden*, Energ. Buildings 261 (2022) 111960.
[45] S.H. Alyami, et al., *Likelihood of reaching zero energy building design in hot dry climate: saudi arabia*, IEEE Access 9 (2021) 167054–167066.
[46] W. Wu, H.M. Skye, *Residential net-zero energy buildings: Review and perspective*, Renew. Sustain. Energy Rev. 142 (2021) 110859.
[47] M.A. Sabbaghi, M. Soltani, M.A. Rosen, *A comprehensive 6E analysis of a novel multigeneration system powered by solar-biomass energies*, Energy 297 (2024) 131209.
[48] A. Nafey, M. Sharaf, *Combined solar organic Rankine cycle with reverse osmosis desalination process: energy, exergy, and cost evaluations*, Renew. Energy 35 (11) (2010) 2571–2580.
[49] E. Assareh, et al., *A proposal on a co-generation system accompanied with phase change material to supply energy demand of a hospital to make it a zero energy building (ZEB)*, Energ. Buildings 318 (2024) 114478.
[50] E. Assareh, N. Agarwal, M. Lee, *Zero energy building optimization for a residential complex with a new optimized cogeneration system for electricity, cooling, heating and freshwater production*, Appl. Therm. Eng. 244 (2024) 122527.
[51] E. Assareh, et al., *Application of PCM in a zero-energy building and using a CCHP system based on geothermal energy in Canada and the UAE*, Buildings 14 (2) (2024) 477.
[52] A. Kusiak, H. Zheng, *Optimization of wind turbine energy and power factor with an evolutionary computation algorithm*, Energy 35 (3) (2010) 1324–1332.
[53] I. Poultangari, R. Shahnazi, M. Sheikhan, *RBF neural network based PI pitch controller for a class of 5-MW wind turbines using particle swarm optimization algorithm*, ISA Trans. 51 (5) (2012) 641–648.
[54] A. Buonomano, et al., *Solar-assisted district heating networks: Development and experimental validation of a novel simulation tool for the energy optimization*, Energ. Conver. Manage. 288 (2023) 117133.
[55] (NREL);, N.R.E.L. BEopt Software. 2024 2024]; Available from: https://www.nrel.gov/buildings/beopt.html.
[56] Meteotest. *Meteonorm Version 8*. 2024 12 December 2024]; Available from: https://meteonorm.com/en/meteonorm-version-8.
[57] T. Kroeger, et al., *Reforestation as a novel abatement and compliance measure for ground-level ozone*, Proc. Natl. Acad. Sci. 111 (40) (2014) E4204–E4213.
[58] A. Nikitin, et al., *Energy, exergy, economic and environmental (4E) analysis using a renewable multi-generation system in a near-zero energy building with hot water and hydrogen storage systems*, J. Storage Mater. 62 (2023) 106794.
[59] F. Rong, et al., *Performance evaluation and multi-objective optimization of hydrogen-based integrated energy systems driven by renewable energy sources*, Energy 313 (2024) 133698.
[60] E. Arslan, et al., *Determining energy, exergy and enviroeconomic analysis of stand-alone photovoltaic panel under harsh environment condition: Antarctica Horseshoe-Island cases*, Renew. Energy 226 (2024) 120440.